Evaluation of Subsurface Impacts on Occurrence of Sand Boils from the 2001 Nisqually Earthquake in the SoDo Neighborhood of Seattle, Washington

Morgan Simon

A report prepared in partial fulfillment of the
requirements for the degree of

Master of Science
Earth and Space Sciences: Applied Geosciences

University of Washington

June 2019

Reading committee:
Kathy Troost
Juliet Crider

MESSAGe Technical Report Number: 075

Executive Summary

The 6.8 magnitude Nisqually earthquake occurred on February 28th, 2001 causing liquefaction in multiple areas of Seattle, mostly in the SoDo neighborhood. Following the earthquake, scientists recorded field observations of the liquefaction in Seattle, which was compiled into a database. While the SoDo neighborhood is mapped as having the same liquefaction potential throughout, large areas did not show above-ground signs of liquefaction, such as sand boils. I looked at the subsurface in areas where sand boils were reported and in areas where no sand boils were reported to determine if significant geologic differences occur in the subsurface that could explain why liquefaction occurred in some areas and not others. The study area has undergone multiple glaciations, and is part of the former Duwamish River delta, occupying a former subglacial trough. In the last century, humans have modified the delta and associated tide flats to expand buildable land by adding variable thicknesses of fill, primarily sourced from nearby glacial deposits. To examine the subsurface, I used the GeoMapNW subsurface database to find borings adjacent to sand boils and borings at sites where sand boils were not reported. I identified target locations, where sand boils did and did not occur, and where good subsurface data are available. I compared the subsurface stratigraphy to depths of 40 feet from selected borings in the target areas and looked at density, sand content and clay content. I also compared the ratio of the thickness of fine-grained sediment to coarse-grained sediment. To compare the densities of the subsurface, I performed clean sand corrections and performed modeling to generate a Liquefaction Potential Index (LPI) at the target locations. I found that areas with capping clay layers at/near the surface of greater than 3ft in thickness or significant amounts of clay within the upper 40 feet were more common in areas where no sand boils were reported. I also found that areas where no sand boils were reported typically had higher ratios of fine-

grained thickness to total thickness, and that these ratios were higher in the eastern portion of the site area. The LPIs at borings adjacent to sand boils were calculated to be high risk or very high risk. The LPIs for the borings chosen in areas where there were no sand boils ranged from low risk to very high risk. Some of the high or very high risk boring locations had caps of clay or near surface layers had undergone construction-related compaction, which may have resulted in liquefaction not reaching the surface and instead potentially spreading laterally. For the Nisqually earthquake the LPI alone does not adequately predict whether or not liquefaction will occur at the ground surface in the SoDo area due to geologic or human-influenced variability. LPI will over predict liquefaction at the ground surface for the SoDo area.

Acknowledgments

Thanks to Dr. Kathy Troost, LG, for coming up with the project, providing accesses to the GeoMapNW database and all of the old Nisqually earthquake documents. And also for reviewing this paper multiple times.

Thanks to Dr. Juliet Crider for reviewing my paper and coming up with new aspects to look at with the data.

Thanks to Vice President Bill Perkins, PE, LEG (Shannon and Wilson), for coming up with the idea that a cap of clay or fines could be worth looking at and that I should preform clean sand corrections on the data.

Thanks to Dr. Brett Maurer for introducing me to the concept of the LPI and teaching me how to calculate it.

Thanks to Mary Alice Benson for reviewing my paper and listening to me complain about ArcMap.

Thanks to the people at Seattle Public Utilities Geotechnical Group for being great coworkers and flexible with me as I finished this project.

Thanks to Sondra-Beck Simon and William Simon for paying my tuition and occasionally buying me groceries.

Table of Contents

List of Figures

List of Tables

1.0 Introduction

In 2001, the magnitude 6.8 Nisqually earthquake shook Western Washington. One result was damage in the form of liquefaction in several parts the Puget Lowland, including the SoDo ("south of downtown") neighborhood in Seattle. In the days shortly after the earthquake scientists coordinated by a University of Washington (UW)/United States Geologic Survey (USGS)/Washington State Department of Natural Resources (WDNR) team recorded field observations of ground failures, including sand boils, caused by the earthquake in multiple areas, including the SoDo neighborhood. Following the collection of data, FEMA (Federal Emergency Management Agency) led an effort to compile the data and create a database (Troost et al., 2001b). The SoDo neighborhood has been mapped as having the same liquefaction potential throughout (Palmer et al., 2004); however the compilation of field observations showed that only some areas of the SoDo neighborhood had recordable evidence of the surface manifestation of liquefaction occurring as a result of the Nisqually earthquake (Troost et al., 2002). While it was hypothesized at the time that the variable degree of compaction may have been a contributing factor to the variable degree of liquefaction (Troost et al., 2001a), more work is needed to fully determine what factors caused liquefaction in only parts of SoDo.

Understanding what geologic factors in the SoDo neighborhood made some areas more susceptible to liquefaction is important to prepare for future seismic events. Seismic events like the Nisqually earthquake occur about every 30-50 years (PNSN, date unknown). The monetary damage associated with the Nisqually earthquake was significant, at least $1 billion (Pierepiekarz et al., 2001).

The goal of my investigation was to determine if differences in the subsurface stratigraphy in SoDo could account for the difference in geographic locations of sand boils. I examined the

characteristics of the shallow subsurface geology by using cross-sections, thicknesses of units less likely to liquefy (such as clay), the amount of sand available for liquefaction, the density of the strata using clean sand corrections, and the calculated liquefaction potential.

2.0 Background

2.1 Geographic Setting

The study site is located within the Puget Lowland, which is an elongate topographic and structural basin between the Olympic Mountains and the Cascade Mountains (Troost and Booth, 2008). The study site is in the SoDo neighborhood of Seattle, WA (Figure 1). This neighborhood includes the right bank of the East Duwamish waterway as it diverges around Harbor Island and enters Puget Sound. The study area is bounded on the on the east by I-5, on the north by Edgar Martinez Dr., on the west by the East Duwamish waterway, and the south boundary is just south of the South Spokane St. Viaduct. This part of the SoDo neighborhood is zoned for primarily industry and business.

2.2 Quaternary Deposition and Erosion

The Puget Lowland has been molded by tectonic processes and at least seven successive glacial and interglacial periods (Troost and Booth, 2008). The most recent period of glaciation was the Frasier Glaciation. During the Vashon Stade of the Frasier Glaciation, the Puget Lobe advanced and retreated from the Seattle region approximately 18,000 to 16,300 cal. yr. B.P. (Booth, 1987; Porter and Swanson, 1998). Puget Sound and other deep valleys were created by subglacial meltwater eroding and creating channels below the Vashon ice sheet (Booth and Hallet, 1993). The present-day Duwamish River is located in a former subglacial trough that joins the Puyallup River trough to the south (Troost and Booth, 2008). With the retreat of the Puget Lobe during the

late Pleistocene, sea level rose, and the Duwamish valley aggraded downstream, creating a large delta of reworked glacial sediment about 30 miles south of Seattle (Dragovich et al., 1994). About 5700 years ago, a lahar known as the Osceola Mudflow, originated from Mt. Rainer and flowed down the White River valley, entered the Green River valley, which eventually entered the Duwamish River valley of the time (Dragovich et al., 1994). The influx of sediment caused aggradation, which eventually formed the modern-day Duwamish River delta. From 5600 to 1000 cal yr. B. P., three other lahars contributed to the filling of the Duwamish trough (Zehfuss, 2005), along with estuarine sediment sourced from the north and alluvial sediment sourced from the south (Troost and Booth, 2008) Tide flats developed on the Duwamish delta (Figure 2), filling occurred, then the SoDo area was built on the new ground.

2.3 Regional Tectonics

The Puget Lowland is tectonically active. The Cascadia subduction zone is west of the Puget Lowland and the Olympic Mountains, where the Juan de Fuca plate is subducting beneath the North American plate. The subduction zone stretches about 600 miles from Northern Vancouver Island to Cape Mendocino, California. As a result of the interaction of crustal blocks in the forearc of Cascadia, the Puget Lowland is also undergoing N-S compression (Wells et al., 1998). The most common form of large earthquakes in the Puget Lowland originates from the deep earthquakes within the subducting Juan de Fuca plate (in the Wadati-Benioff zone), which occur about every 30-50 years (PNSN, date unknown). The most active part of the Juan de Fuca Wadati-Benioff zone is beneath the forearc of northwestern Washington (Weaver and Baker, 1988), beneath the Puget Lowland. The study site lies within a shallow crustal fault zone known as the Seattle Fault Zone (Pratt et al., 2015). This fault zone is capable of producing magnitude 7.0 earthquakes (Nelson et al., 2014). A third important seismic source is the subduction zone

itself. Magnitude 8.5 and greater earthquakes are produced along the subduction zone, known as "megathrust" earthquakes, with the last one in the region occurring in 1700 (Nelson et al., 1995). These earthquakes occur about every 400 to 600 years (PNSN, date unknown).

On the 28th of February 2001, a magnitude 6.8 earthquake with an epicenter 32 miles beneath the Nisqually River delta, shook the Puget Lowland. The peak accelerations ranged from about 0.04g to 0.31g (Frankel at al., 2002). Liquefaction occurred in areas containing poorly compacted fill, alluvial valleys and river deltas (Troost et al., 2001a). Extensive liquefaction was observed in the industrial area in the Duwamish waterway and along the eastern runway of Boeing Field (Troost et al., 2001a; Figure 3). At the time of the earthquake three strong-motion stations, known as the SD array, were located in SoDo (Frankel, et al., 2002). The SD array was composed of the stations SDS, SDW, and SDN. A peak ground acceleration of 0.28g was recorded at the SDS and SDW stations, both of which were near reported liquefaction from the earthquake. Other ground failures reported include settlement, lateral spreading, and ground cracks (Malone et al., 2001).

Prior to the Nisqually earthquake, several other large Benioff zone earthquakes occurred in the region. On April 13th, 1949 a 7.1 magnitude earthquake occurred near Olympia and on April 29th, 1965 a 6.5 magnitude earthquake occurred about 14 miles south of Seattle (Weaver and Baker, 1988). From the 1949 earthquake, an area of about 11,000 square miles experienced scattered ground failures (Chleborad, 1988). In both earthquakes, structural damage was substantial in the former Duwamish tide flats area. Sand boils were reported in the SoDo area produced by both earthquakes. In addition, other forms of liquefaction such as lateral spreading and settlement were reported in the SoDo.

2.4 Site History

Starting in the late 1800s and continuing to about 1930, the landscape of Seattle was altered through extensive excavation and filling. The Duwamish River delta tide flats (Figure 2) were reclaimed for industrial use by regrading primarily by sluicing from adjacent uplands, such as Beacon Hill (Phelps, 1978; Troost and Booth, 2008). The regrades resulted in the mouth of the Duwamish River being extended about half a mile northwest to the present location (Phelps, 1978). The Duwamish River was also straightened into the modern-day Duwamish Waterway beginning in 1913 and dredged material from the straightening was added to the tide flats. Additional sediment was added to the Duwamish delta from the Jackson and Dearborn Regrades (Grant et al., 1991). For the next century, the area was used for primarily industrial use. Prior to the 1970s, most of the fill was not compacted or monitored for quality of materials, resulting in variable density and composition (Troost and Booth, 2008).

2.5 Previous Work

Grant et al. (1991) is the first published evaluation of the liquefaction potential in Seattle. Their methodology involved using boring logs to evaluate the potential liquefaction through two procedures. The first procedure grouped similar geologic units and assigned the groups liquefaction potential relative rankings based on the density determined by Standard Penetration Test (SPT) N-values and a threshold N-value needed to resist liquefaction from an earthquake resulting in 0.30g ground acceleration. The second procedure assigned liquefaction potential rankings based on the computed thickness of sediment in individual borings that would liquefy for ground accelerations of 0.15g and 0.30g. Their evaluation used empirical relations developed

by Seed and Idriss (1971) and Seed et al. (1983 and 1984). They determined that the liquefaction potential in the former Duwamish River tide flats was high.

3.0 Methods

3.1 Liquefaction Database

Following the Nisqually earthquake, a UW/UGGS/WADNR team coordinated scientists to collect field observations across the central Puget Lowland and record observations of ground failures, such as sand boils (Figure 4) and lateral spreading (Troost et. al., 2001b). To create a database of the recorded instances of liquefaction, FEMA facilitated the data compilation into an ArcView layer. Over the last decade the responsibility of handling the database changed hands and at some point the electronic database was lost (K Troost, personal communication, 2018). A paper copy of the original ArcView attribute table for the database was found as well as various notes, including field notebooks. Using these notes and the paper copy of the attribute table I recreated most of the database for the SoDo neighborhood in ArcMap, mapping where sand boils were observed (Figure 5). The term "sand boils" will be used to refer to areas where liquefaction was expressed at the ground surface. The Create Features tool was used to place each point were a sand boil was reported and the editor tool was used to edit information into the corresponding attribute table. Some sand boils were not added to the database due to insufficient location information in the paper table and notes, which limited the data usable for the study. Multiple sand boils may be represented by one point as illustrated in Figure 6.

3.2 Boring Log Database

The primary source of data for this investigation was boring logs for the Seattle area compiled in the GeoMapNW database (subsurface database, University of Washington, date accessed:

September 2018). This database includes mapped locations for all of the explorations in the database and attribute tables for each layer recorded in the boring logs. I entered groundwater data and SPT data into the database using the editor tool in ArcMap following protocols developed for GeoMapNW. For the groundwater table I entered if groundwater was encountered, the depth of the groundwater, the date that the groundwater depth was recorded, the type of observation, and if there were multiple groundwater depths within a single boring (such as perched groundwater). For the SPT table I entered the layer that the blow count was associated, depth of the blow count, if it was an SPT or other split spoon sample type, blow count for each six inches, refusal and penetration depth when appropriate, the sampler type, diameter in inches, diameter type, hammer type, and drop inches. For some logs instead of the blow counts being listed per six inches, the N-value was given, which was then divided in two and listed as the 2nd and 3rd blow counts. Within the database, there were about 1100 explorations in the study area. Boring logs that gave a location confidence of greater than 100 ft were not used. If the blow counts were not done to the strict SPT standards or could not be determined if they were done to strict SPT standards, the blow counts were not used in my work and were not entered into the database.

3.3 Visual Analysis

To gain an understanding of the subsurface, I used the Geologic Cross Section Tool (Schaefer et al., 2018) in ArcMap to generate multiple cross-sections of the subsurface (Figure 7). The cross-sections were used for reconnaissance and to see if there were any easily noticed patterns in the subsurface. Several long cross-sections were created trending north-south and east-west across the study area. Cross-sections were also created along multiple sand boil points and in areas where no sand boils were recorded. A cross-section was generated for each sand boil to evaluate

the subsurface at and away from the sand boil. Cross-sections were also generated in areas with no recorded sand boils to examine the subsurface.

3.4 Selection of Target Areas

I selected target areas to focus my study for areas with and without sand boils. Criteria for selection included having borings deeper than 20 feet with high location confidence, good descriptions of the units, and where borings were close to areas with and without sand boils. In Excel, the thickness, density, Unified Soil Classification System (USCS) and major and minor components of each unit were recorded for the nearest boring to each sand boil. Not all sand boils had borings close enough (less than 150ft) to use in my study. In some cases, shallow borings (less than 30ft) were closer to the sand boil location than deeper borings, but I used the deeper borings if the initial stratigraphy agreed with the shallower borings and were still within a 150-ft radius. Because not all of the reported sand boils had nearby boring logs to evaluate the subsurface, I was limited in the amount of sand boil data I could use. I used twenty-six borings adjacent to sand boils (Figure 8). I also used twenty-two borings in areas without sand boils (Figure 9). Combined this gave a total of forty-eight target areas.

3.5 Fine-Grained Caps

I evaluated the borings in the target areas to look for differences between where sand boils were and were not observed. One factor of interest in the subsurface was whether or not a fine-grained layer exists near the surface. I defined a capping layer as beginning no deeper than 15ft below the surface and being at least 3ft thick. Using the thickness and USCS, I recorded the presence and thickness of surficial fine-grained layers (silt and/or clay). In addition, I determined a ratio of

fine-grained thickness to total thickness of substrate materials in borings for each target area. I also recorded caps of only clay and a ratio of clay thickness to total thickness.

3.6 Clean Sand Correction

The density of layers in the subsurface at target areas was also compared. To compare the densities, a clean sand correction was determined for each SPT N-value, known as the $(N_1)_{60cs}$, using the 2014 CPT- and SPT-based liquefaction triggering procedures of Boulanger and Idriss (2014). The clean sand correction is the SPT N-value removes the influence of fines and accounts for the effects of overburden pressure to allow more accurate comparisons between the densities of different units. I focused on the upper 40ft of the subsurface at borings based on the depth used by Grant et al. (1991) for their evaluation of the liquefaction potential in Seattle. To determine the clean sand correction, I extracted the percent fines content, the SPT N-value, and depth of the N-value from each boring log. I corrected each SPT N-value at target locations that had grain size data with percent fines, or that had detailed enough descriptions to give reasonable estimates on the fines content. I then used Excel to perform the calculations following Boulanger and Idriss (2014). To check the $(N_1)_{60cs}$ calculations I also used the LiqSVs 2.0 software (https://geologismiki.gr/products/liqsvs/#requirements3598-c4ca), a liquefaction analysis software that uses SPT data, by GEOLOGISMIKI, with the same data used for Excel. Excel was used to plot the histograms of the clean sand corrections. Of the nine sand boils that had associated boring logs with sufficient grain size information, I used eight (Figure 10). I did not use one due to a large gravel and concrete debris layer within the subsurface: the log notes that the concrete debris likely skewed the measured density to be higher than it actually is. For the areas without sand boils, I calculated equivalent "clean sand" densities for twenty-two borings (Figure 9).

3.7 LPI Model

I calculated the liquefaction susceptibility of the subsurface using Boulanger and Idriss (2014) and the Liquefaction Potential Index (LPI; Iwasaki et al., 1978) in Excel and in LiqSVs 2.0. Input to these calculations include: the percent fines content, SPT N-values, the depth of groundwater, magnitude of the earthquake and peak ground acceleration. Groundwater depth was obtained from the boring logs and from other logs in the immediate vicinity based on the dates of the recorded groundwater, with late winter preferred. The peak ground acceleration for the Nisqually earthquake was 0.28g in the study area (Frankel et al., 2002).

If the Plasticity Index of a unit is greater than 12, the unit will not typically liquefy (Boulanger and Idriss, 2006). In general, if the unit was designated CH, I assumed that it was non-liquefiable. In the LiqSVs program the 'Can Liquefy' box for the N-value in question in the data input table was unchecked for any layers described as "CH" in order to properly do the calculations. I did this in Excel by manually changing the values that are automatically changed in LiqSVs. In some borings logs the plasticity index of clayey units was given. In others I made a judgment call on the plasticity index based on the description of the unit.

LiqSVs models the factor of safety with depth using the Boulanger and Idriss (2014) method and models the LPI with depth using Iwasaki et al. (1978). LiqSVs also plots the clean sand curve that separates the N-values for layers that can liquefy and cannot liquefy in a given earthquake scenario. The values generated by LiqSVs were cross-checked using my Excel calculations based on the two methods. The same borings used for the clean sand correction were used for the LPI (Figures 9 and 10).

4.0 Observations and Analyses

4.1 Subsurface Characteristics

Overall, the subsurface of the site is heterogeneous with fill overlying tide flat and deltaic deposits. Fill thickness reported on boring logs ranged from 5ft to 30ft. For the fill, clean sandy layers, silty sandy layers, silt layers, clay layers, gravely sandy layers, mixed silt and clay layers, mixed sand and clay or silt layers, and layers of cinders or other garbage were all common in the subsurface. Brown, shades of gray, and black were all common colors associated with the fill. For the tidal/deltaic deposits, clean sandy layers were the most common but silty sandy layers, silt layers, clay layers and mixed silt and clay layers were also all common. Red and black sand grains were also common and the layers tended to be shades of gray or brown. Trace gravel was present and bioturbation was sometimes present. In deeper borings, the tidal/deltaic deposits had thicknesses from 40ft to over 150ft. Organics such as shell fragments, wood, and rootlets were found in layers designated as fill and in tidal/deltaic layers. Whether the layer was fill or tidal/deltaic deposits was not always noted in the boring logs. Layers where sand was the major component were the most common in the subsurface. Ground water was typically 10ft or less below the surface, but up to 15ft below surface in the east portion of the site. There are extensive buried utilities in the neighborhood. The ground cover in the neighborhood is variable as well. In some locations, concrete was as thick as 2ft to 3ft. More common was about a half a foot of concrete or asphalt with several inches of crushed gravel beneath. In other areas, such as railyards, the ground surface was dirt. Buildings are also present throughout the site area.

There were several modes of fill deposition that may have contributed to the variability as well. One mode was sluicing from hydraulic erosion, which sourced material primarily from the regrades (Morse, 1989). Parts of the tide flats were purposely filled to an elevation of 12ft below

the final grades at the time for future sanitary landfill operations. Dredged material from the straightening of the Duwamish waterway was also dumped in the tide flats, starting in 1895 (Phelps, 1978). Another mode of fill deposition in the tide flats was garbage dumping. A slow fire was typically kept burning to destroy any combustibles in the waste. In addition, some areas have been redeveloped over the years, which would contribute to variable fill compaction over short distances.

4.2 LPI Model

I determined the LPI on the subsurface data adjacent to eight sand boils (Figures 11 and 12). The LPI produces three categories of risk: low risk, high risk and very high risk. Low risk is calculated to be below 5, high risk is between 5 and 15 and very high risk is above 15. Three of the boring locations for the sand boils were calculated to be high risk and the other five were calculated to be very high risk in the Nisqually earthquake scenario. The boring near Sand Boil 36 was on the border between high risk and very high risk. The lowest LPI calculated was 10 and the highest was 27.

I determined the LPIs for twenty-two borings at sites without sand boils (Figures 11, 13). Each boring location selected for target areas without sand boils was given a designation NSB- (No Sand Boil #). Five of the NSB boring locations were calculated to be of low risk to liquefaction in the Nisqually Earthquake scenario; seven of the NSB boring locations were calculated to be of high risk; and ten of the NSB boring locations were calculated to be of very high risk (Figure 13). The LPI at NSB9 was determined to be at the border between low and high risk. The LPI at NSB2 was determined to be at the border between high and very high risk. The lowest LPI calculated was less than one and the highest was thirty-four.

4. 3 Fine-Grained Cap

Forty-six percent of the borings with sufficient subsurface information near reported sand boils had a cap of fine-grained sediment near the surface (Table 1).

Table 1- Table showing the prevalence of a fine-grained cap at target locations.

	With Sand Boil	Without Sand Boils
Clay Cap	15%	41%
Fine-Grained Cap (silt and/or clay)	46%	64%
No Cap	54%	36%

Out of this 46%, 15% had a cap of clay near the surface. Sixty-four percent of the boring locations with no recorded sand boils had caps of fine-grained sediment near the surface. Out of this 64%, 41% of the boring locations had a cap of clay near the surface. The thickness and depths of fine-grained layers are presented graphically on stick logs for the borings used in the target areas used for the LPI determinations (Figure 14). In general, the higher the fines thickness ratio, the lower the LPI (Figure 15). In general, the higher the clay thickness ratio, the lower the LPI (Figure 16). In both cases the ratios of fine-grained or just clay is greater for the boring locations used for sites without sand boils than the boring locations used for sites with sand boils. Spatially, the sites with higher fine-grained thickness tend to be on the eastern side of the study area (Figure 17), with a large concentration in the northeast section of the study area, with the fine-grained thickness decreasing westward.

4. 4 Corrected density (‘clean sand’ correction)

I compared all of the clean-sand-corrected SPT N-values for the borings associated with sand boils (Figure 18). For the modeled sand boils, the majority of the densities are in the loose to

medium-dense range. Similarly, for the borings without associated sand boils, the majority of the densities are in the loose to medium-dense range (Figure 19). However, the histogram for sites without sand boils shows a gentler decline in the frequency of corrected SPT N-values when increasing in density.

I also compared depth versus density for the clean sand corrections of two borings at sand boils (Figure 20). The boring nearest Sand Boil 4, with the lowest LPI of the sites with sand boils, has corrected density values mostly in the medium dense category. A cap of fines was also present at this location. The boring nearest Sand Boil 33, with the highest LPI of the sites with sand boils, has mostly densities in the loose or medium dense category. A cap of fines was not present at this location.

Graphs of the corrected density with depth for some borings without sand boils were also compared based on the LPI and the absence of a fine-grained cap. Two locations with fine-grained caps were also compared (Figure 21). NSB1, with a LPI of low risk and consisting mostly of silt, is medium dense for the upper 40ft (Figure 21). NSB19, which also has a low risk LPI and a thin fine-grained cap, is mostly medium dense in the upper 40ft (Figure 21). Boring location NSB12 (Figure 22) has no fine-grained cap, has a very high risk LPI, and is loose through the upper 40ft and dense near the surface. Boring location NSB16 (Figure 22), also with a LPI of very high risk and no fine-grained cap is dense near the surface and very loose to medium dense through the upper 40ft. The other borings for sites without sand boils, but had high or very high LPIs and had no fine-grained caps were also compared (Figure 23) to show the distribution of densities for these sites. Borings NSB6, NSB8, NSB17, and NSB20 all have the same trend of being mostly medium dense for the upper 40ft. Boring NSB3 is mostly loose to

medium dense for the upper 40ft. Three of these sites; NSB3, NSB17, and NSB20; were dense near the surface.

5.0 Discussion

Not all the sand boils were mapped due to poor location information. It is also likely that other sand boils were formed but not found during the post-earthquake reconnaissance (K. Troost, personal communication, 2019). Some liquefaction occurred in the subsurface and caused sand to enter utility trenches and basements (K Troost, personal communication, 2019). So while this study looked at above-ground liquefaction (sand boils), subsurface liquefaction that did not reach the surface may have occurred in the areas I identified as not having sand boils. Also, some of the sites without sand boils might have already liquefied during the 1949 and 1965 deep earthquakes but the exact locations are unknown.

Although it was initially expected that the sites without sand boils would have LPI values of low risk, the modeling produced LPIs from all three risk categories for the sites without sand boils. For the sites without sand boils I looked for the presence of a fine-grained cap. Of the nine sites without sand boils that had LPIs of very high risk (Table 2), five had fine-grained caps near the surface, four of which were clay caps. Of the remaining four sites, three were dense near the surface and one had 2ft of concrete at the surface.

Table 2- Summary table for NSB sites with very high risk LPIs.

Site number #	Fine-Grained Cap	Dense Near Surface	Other	Comments
NSB - 2	X			Cap is clay
NSB - 5	X			Cap is clay
NSB - 6			X	2ft concrete on top

NSB - 12		X		
NSB - 15	X			Cap is clay
NSB - 16		X	X	Bottom half is clay and silt
NSB - 18	X			Cap is silt
NSB - 20		X		
NSB - 21	X			Cap is clay

For the eight sites without sand boils that had LPIs of high risk (Table 3), five had fine-grained caps near the surface, four of which were clay caps. Of the remaining three, two were dense near the surface and one was mostly medium dense and dense in the upper 40ft.

Table 3- Summary table for NSB sites with high risk LPIs.

Site number#	Fine-Grained Cap	Dense Near Surface	Other	Comments
NSB - 3		X		
NSB - 4	X			Cap is clay
NSB - 7	X			Cap is clay
NSB - 8			X	Mostly medium dense and dense
NSB - 9	X			Cap is silt
NSB - 12	X			Cap is clay
NSB - 14	X			Cap is clay
NSB - 17		X		

Three of the five sites without sand boils that had LPIs of low risk (Table 4) had clay caps. One of the boring locations (NSB1) was all silt beginning 9ft below the surface and another (NSB19) had a cap of silt and the layers were mostly medium dense to dense in the upper 40ft.

Table 4- Summary table for NSB sites with low risk LPIs.

No Sand Boil#	Fine-Grained Cap	Dense Near Surface	Other	Comments
NSB - 1	X			70% of boring is silt
NSB - 10	X			Cap is clay
NSB - 11	X			Cap is clay
NSB - 19	X			Cap is silt, mostly medium dense and dense layers
NSB - 22	X			Cap is clay

Because clay is not typically a liquefiable material, except with very low plasticity indexes (Boulanger and Idriss, 2006), it is possible that in the eight cases of sites without sand boils with high or very high risk, the clay layer prevented liquefaction from reaching the ground surface if liquefaction occurred. If the silt was thick enough or had a high enough plasticity, it might have also prevented liquefaction from reaching the ground surface. The plasticity index was typically not recorded in the available boring logs. And while there were caps of clay or silt associated with some of the sand boils, the percent of borings with fine-grained caps near the surface were greater for the areas with no reported sand boils, 46% versus 64% in the case of fines or 15% to 41% in the case of clay. In addition to this large difference in clay caps between sites with sand boils and sites without sand boils, most of the fine-grained caps seen at the sites without sand boils were clay. This could indicate that having a clay cap was one of the stronger factors in preventing surficial liquefaction in the Nisqually Earthquake.

While most of the sites without sand boils did have a cap of fines, some of the sites did not. Of the four sites without sand boils that were rated as being very high risk (Table 2) and didn't have a fine-grained cap, three were dense at or near the surface, and the last had 2ft of concrete at the surface. One of the sites that had a dense cap was also silt and clay for the lower 20ft to 40ft of the boring. Of the three sites without sand boils that were rated as being high risk (Table 3) and didn't have a fine-grained cap, two were dense at or near the surface. The other site was mostly medium dense and dense for the upper 40ft. Having near surface compacted layers, resulting in high density, may have also prevented liquefaction from reaching the surface, and instead potentially spreading laterally through the subsurface. In one case, NSB6, with low fines content

and primarily medium dense layers, 2ft of concrete was at the surface, which may have prevented liquefaction from reaching the surface.

I also took a closer look at the borings associated with sand boils to determine why the LPI expected these sites to liquefy. The boring associated with Sand Boil 4, which had the lowest LPI of the sand boils, did have a 9ft section of clay about 15ft below the surface, but the clay was bounded by sandy units above and below that had density values mostly less than an N-value of 20. Borings associated with Sand Boil 8 and Sand Boil 36 had thin, about 5ft, deeper layers of clay than Sand Boil 4. And in the case of the boring associated with Sand Boil 8, the water level was also reported as being about 3ft below ground surface, so it is possible that either the clay layer was liquefiable or the liquefaction occurred above the clay layer. The boring associated with Sand Boil 33 did have a dense layer near the surface, but was mostly loose and low to medium dense and was primarily sand.

The overall thickness of fines in the upper 40ft (Figure 15) may also have affected the presence of sand boils. The lower LPIs tended to have higher ratios of fine-grained thickness to total thickness; the same pattern also occurred for the ratio of clay-thickness to total thickness (Figure 16). The sites without sand boils also had thicker fine-grained layers than the sites with sand boils.

The occurrence of sand boils in the study area may also show spatial variability. The majority of the sand boils occurred below 20ft in elevation (Figure 5). The distribution of fines-to-total thickness ratio shows higher fines content to the east and decreasing westward (Figure 17). This could signify that fine-grained fill was deposited closer to the former shoreline of the tide flats (Figure 2) or that coarser sediments were less likely to be deposited near the eastern extent of the

tide flats and delta. The finer-grained nature of the eastern portion of SoDo could be less susceptible to liquefaction.

While the LPI model was able to predict liquefaction occurring at each of the sites of reported sand boils, the model was less useful when looking at the sites where sand boils were not reported. For the sites with sand boils, the LPI was rated as being high or very high risk. Most of the sites without sand boils also had LPIs of high to very high risk. This suggests that the LPI calculations that I used cannot discriminate among sites with variable substrate in SoDo. I think there are three reasons why this may be so. One, while the model is originally based on a 7.5 magnitude earthquake, it does correct for the actual magnitude of the earthquake. However, it is possible that despite the corrections, a 6.8 magnitude earthquake is not suitable for this type of model. Two, it is also possible that the unique nature of the subsurface for the site area is not suitable for this type of modeling, despite its worldwide use, due to the decades of human modification through the use of engineered and unengineered fill. The LPI modeling could be more useful for determining which areas require further investigation for liquefaction hazard. Three, maybe liquefaction happened in the subsurface, but was not observed, due to fine or dense caps that prevented the liquefaction from reaching the surface.

6.0 Recommendations for Further Work

One recommendation I have for further work would be to create 3D models of the subsurface in the study area to further visualize the differences in the subsurface. This could help determine if there is a spatial distribution of large amounts of fines in the subsurface. I would also recommend further work in liquefaction susceptibility modeling for the area using the different models that are available. This could help validate the modeling already done for this study. It

may also be worth repeating my study methods but using a different field area with well recorded liquefaction to determine if the procedures done in this study are viable. Another possibility for additional work would be to test scenarios of different earthquake magnitudes and peak ground accelerations to see how that changes the LPI. Collecting the available CPT data or obtaining new CPT and running the same comparisons could also be worthwhile to see if the boring method or soil classification, such as determining if the unit is silt or clay in the field, causes significant differences.

7.0 Conclusions

The goal of my investigation was to determine if differences in the subsurface stratigraphy in SoDo could account for the difference in geographic locations of sand boils. I examined the characteristics of the shallow subsurface geology by using cross-sections, thicknesses of units less likely to liquefy (such as clay), the amount of sand available for liquefaction, the density of the strata using clean sand corrections, and the calculated liquefaction potential. Overall, I determined that the presence of a fine-grained cap had some control on the presence of sand boils. This could also suggest that capping the subsurface with clay or silt could prevent liquefaction from making it to the surface in certain earthquake scenarios. However, a fine-grained cap is not an absolute determining factor on whether sand boils will reach the surface due to the presence of fine-grained caps at some sand boil locations. Due to the significant difference between clay present (15% vs 41%) at the boring locations where sand boils were reported and the boring locations where sand boils were not reported, clay content likely was a strong factor in surficial liquefaction from the Nisqually Earthquake. The results of my methods show that the subsurface in the study area is heterogeneous in grain size, fines content/thickness,

density, and surface cover. More sophisticated methods are required to determine area-wide LPI in such conditions. I propose using the LPI to determine the initial liquefaction hazard posed at a site and if the site rates higher than a low risk do further investigation of the subsurface or more detailed liquefaction modeling. My findings show that layer density is not a good method on its own to determine whether or not liquefaction will reach the ground surface. However, I still recommend evaluating layer density since thick dense layers are known to be resist liquefaction. Corrected density of the upper 40ft and calculated LPI do not help discriminate between areas with reported sand boils and areas without reported sand boils in SoDo. It is unclear whether the areas without sand boils did not liquefy or if a clay cap prevented liquefied materials from reaching the ground surface.

9.0 References

Booth, D.B., 1987, Timing and processes of deglaciation along the southern margin of the Cordilleran Ice Sheet. North America and Adjacent Oceans during the Last Deglaciation: Boulder. Colorado, Geological Society of America. Geology of North America. v. 3. p. 71-90.

Booth, D.B., and Hallet, B., 1993, Channel networks carved by subglacial water: Observations and reconstruction in the eastern Puget Lowland of Washington, Geological Society of America Bulletin. v.105. p. 671-681.

Boulanger, R.W., and Idriss I.M., 2006, Liquefaction susceptibility criteria for silts and clays, Journal of Geotechnical and Geoenvironmental Engineering, v. 132, no. 11.

Boulanger, R.W., and Idriss I.M., 2014, CPT and SPT based liquefaction triggering procedures, Center for Geotechncial Modeling, Department of Civil and Environmental Engineering, University of California, Davis, California, UCD/GCM-14/01.

Chleborad A.F., Schuster, R.L., 1998, Ground failure associated with the Puget Sound region earthquakes of April 13, 1949, and April 29, 1965, *in* Rogers A.M., Walsh T.J., Kockelman W.J., Priest G.R., eds., Assessing earthquake hazards and reducing rick in the Pacific Northwest, v. 2, U. S. Geological Survey Professional Paper 1560, p. 373-440

Dragovich, J.O., Pringle. P.T., and Walsh. T.J., 1994. Extent and geometry of the mid-Holocene Osceola Mudflow in the Puget Lowland: Implications for Holocene sedimentation and paleogeography: Washington Geology, v. 22. p. 3- 26.

Frankel, A.D., Carver D.L., and William R.A., 2002, Nonlinear and Linear Site Response and Basin Effects in Seattle for the Nisqually, Washington, Earthquake, Bulletin of the Seismological Society of America, v. 92, no. 6, p. 2090–2109

Grant, P.W., Perkins, W.J., and Youd, T.L., 1991, Evaluation of Liquefaction Potential in Seattle, Washington, U.S. Geological Survey Professional Paper 1560, P. 441.

Iwasaki, T., Tatsuoka, F., Tokida, K.I., and Yasuda, S., 1978, A practical method for assessing soil liquefaction potential based on case studies at various sites in Japan, Fifth Japan earthquake engineering symposium, 1978, Issue 5, pp. 641-648

Malone, S., Crosson, B., Creader, K., Qamar T., Thomas, G., Ludwin, R., Toost, K., Booth, D., and Haugerud, R., 2001, Preliminary Report on the Mw = 6.8 Nisqually, Washington Earthquake of 28 February 2001. Seismological Research Letters; v. 72, no. 3, p. 352–361

Morse, R.W., 1989, Regrading Years in Seattle, Engineering Geology in Washington, v. 2, b. 78, p. 691-701

Nelson, A.R., Atwater, B.F., Bobrowsky, P.T., Bradley, L., Clague, J.J., Carver, G.A., Darlenzo, M.E., Grant, W.C., Krueger, H.W., Sparks, R., Stafford, T.W., Stulver, M., 1995, Radiocarbon evidence for extensive plate-boundary rupture about 300 years ago at the Cascadia subduction zone, Nature, v. 378, no. 23

Nelson, A.R., Personius, S.F., Sherrod, B.L., Kelsey, H.M., Johnson, S.Y., Bradley, L., Wells, R.E., 2014, Diverse rupture modes for surface-deforming upper plate earthquakes in the southern Puget Lowland of Washington State, Geosphere, v. 10, n. 4

Pacific Northwest Seismic Network, "Cascadia Subduction Zone", https://pnsn.org/outreach/earthquakesources/csz, accessed 1/21/2018

Palmer, S.P., Magsino, S.L., Bilderback, E.L., Poelstra, J.L., Folger, D.S., and Niggemann R.A., 2004, Liquefaction susceptibility map of King County, Washington; Washington Division of Geology and Earth Resources Open-File Report 2004-20, scale 1:150,000, 1 sheet.

Pratt T.L., Troost, K.T., Odum, J.K., Stephenson, W.J., 2015, Kinematic of shallow backthrusts in the Seattle fault zone, Washington State, Geosphere, v. 11, no. 6, p. 1948-1974

Phelps, M.L., 1978, Public works in Seattle: A narrative history of the Engineering Department 1875-1975, Seattle Engineering Department, 304 p.

Pierepiekarz, M.R., Ballantyne, D.B., and Hamburger, R., 2001, Damage Report from Seattle, Civil Engineering, v. 71, no. 6, p. 78.

Porter, S.C. and Swanson, T.W., 1998, Radiocarbon age constraints on rates of advance and retreat of the Puget Lobe of the Cordilleran Ice Sheet during the last glaciation, Quaternary Research, v. (50) 3, p.205-213

Schaefer, J., Schwitters D., Weiser, M., 2018, Geologic cross section toolbox instructions and cross section tool, UW MGIS program Capstone Report, 17 p., GeologicScrossSectionToolbox_v1.

Seed, H.B., and Idriss, I.M., 1971, Simplified procedure for evaluation soil liquefaction potential: Journal of the Soil Mechanics and Foundations Division, American Society of Civil Engineers, v. 97, p. 1249-1273.

Seed, H.B., Idriss, I.M., and Arango. I., 1983, Evaluation of liquefaction potential using field performance data: Journal of Geotechnical Engineering, American Society of Civil Engineers, V. 109, p. 458-482.

Seed, H.B., Tokimatsu, K., Harder, L.F., and Chung, R.M., 1984, The influence of SPT procedures in soil liquefaction resistance evaluations: Berkeley, California, University of California UCB/EERC-84/15.

Troost, K.G., Booth, D.B.; Shimel, S.A., and Frankel, A.D., 2002, Geologic controls on site response and ground failures in Seattle during the 2001 Nisqually earthquake, Seismological Research Letters, v. 73, no. 2, p. 214.

Troost, K.G., Booth, D.B., Shimel, S.A., Haugerud, R.A., Kramer, S.L., Kayen, R.E., and Barnhardt, W.A., 2001a, Geologic controls on ground failures in Seattle and vicinity during the 2001 Nisqually earthquake, Seismological Research Letters, v. 72, no. 3, p. 393.

Troost, K.G., Haugerud, R.A., Walsh, T.J., Harp, E.L., Booth, D.B., Steele, W.P., Wegmann, K.W., Pratt, T.L., Sherrod, B.S., and Kramer, S.L., 2001b, Ground failures produced by the Nisqually earthquake, Seismological Research Letters, v. 72, no. 3, p. 396.

Troost, K.G., and Booth, D.B., 2008, Geology of Seattle and the Seattle area, Washington, *in* Baum, R.L., Godt, J.W., and Highland, L.M., eds., Landslides and engineering geology of the Seattle, Washington area: Geological Society of America Reviews in Engineering Geology, v. XX, pp. 1-35

Thompson, A.H., McKee, R.H., and U.S. Coast and Geodetic Survey, 1894, Washington, Seattle Sheet: U.S. Geological Survey, scale 62,500, 1 sheet

Wells, R.E., Weaver, C.S., Blakely, R.J., 1998, Fore-arc migration in Cascadia and its neotectonic significance, Geology, v. 26, no. 8, p. 759-762.

Weaver, C.S., and Baker, G.E., 1988, Geometery of the Juan de Fuca plate beneath Washington and northern Oregon from seismicity, Bulletin of the Seismological Socity of Maerica, v. 78, no. 1, p. 264-275

Zehfuss, P.H., 2005, Distal records of sandy Holocene lahars from Mount Rainier [PhD. dissertation]: University of Washington, Seattle, 160 p.

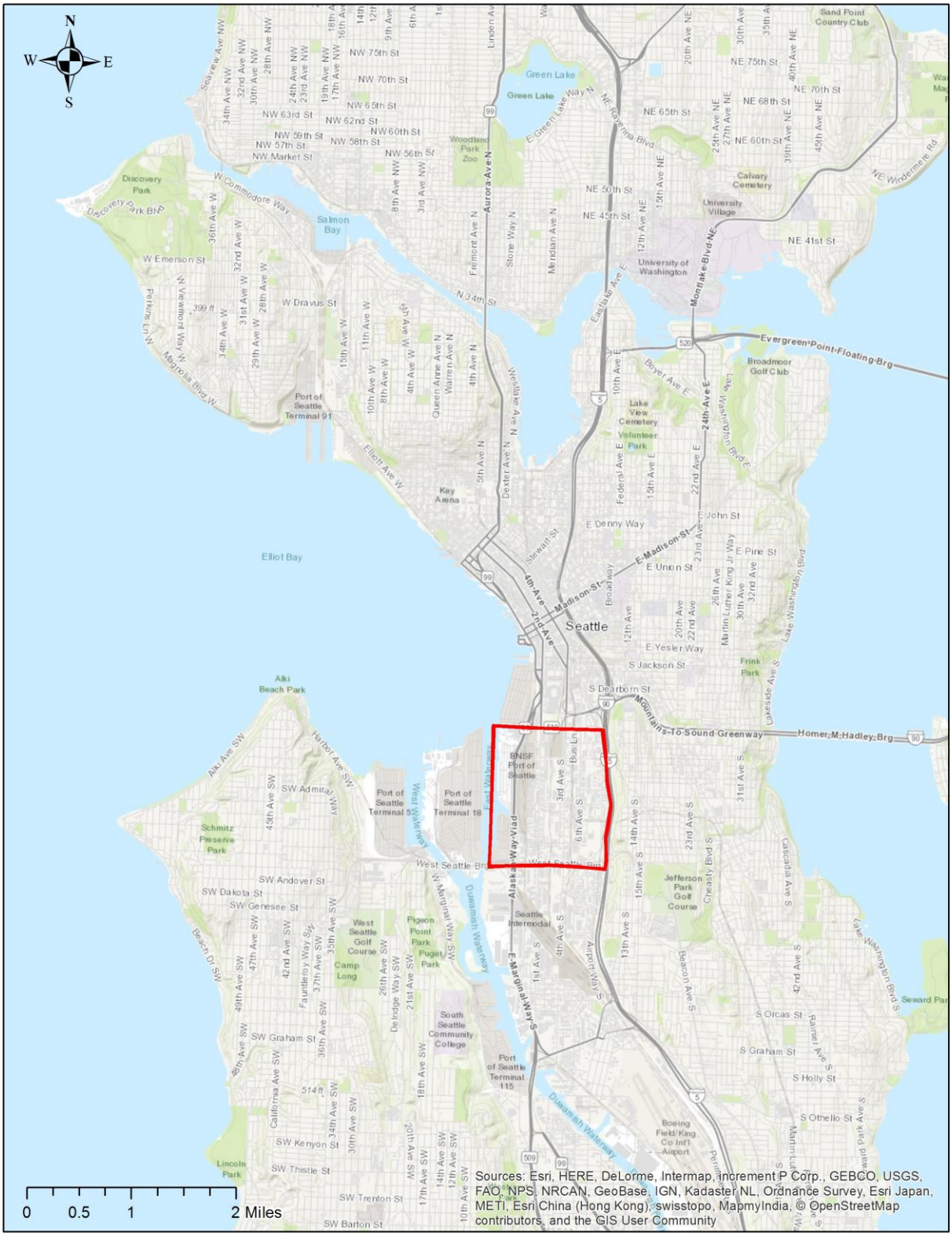

Figure 1- Location map of Seattle, WA showing the site area outlined in red.

Figure 2- Historic USGS topographic map of Seattle showing the Duwamish River Delta, surveyed in 1893 (Thompson, et al., 1894). Red circle shows tidal and delta area.

Figure 3- Photo of sinkhole and sand boils at Boeing Field following the Nisqually earthquake. Half of Kathy Troost for scale. Photo provided by Kathy Troost.

Figure 4- Photo of sand boils (location 7) south of T-Mobile Park in the railyard between S Massachusetts St and S Holgate St. Photo provided by Kathy Troost.

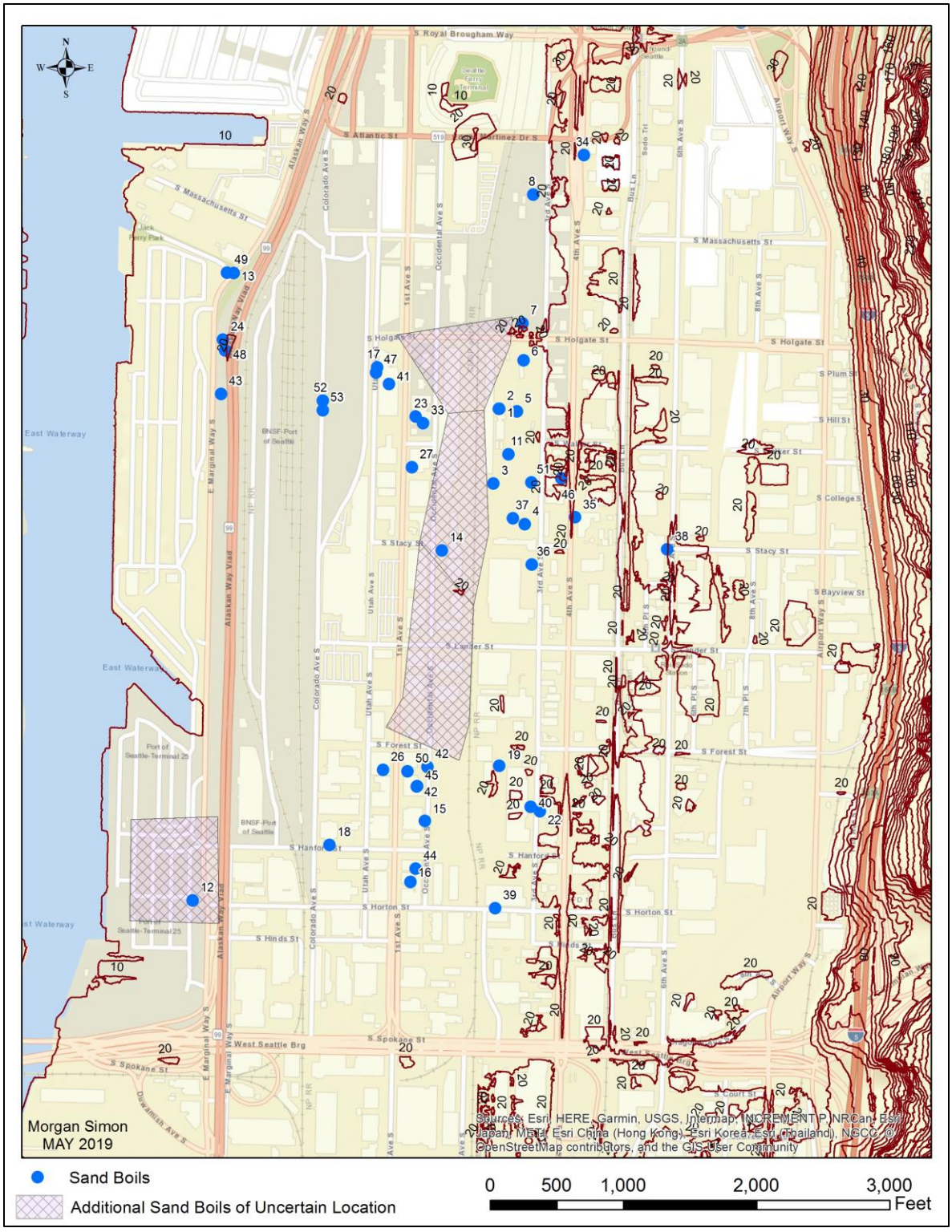

Figure 5- 10ft contour map showing the locations of reported sand boils following 2001 Nisqually Earthquake. Sand boils are symbolized by the blue dots and are labeled according to the number that they are referred to throughout the text. Multiple sand boils may be represented by one dot. The light purple cross-hatch represents areas where additional sand boils were reported but with insufficient location information to accurately plot.

Figure 6- Photo showing multiple sand boils at one location. Pen for scale. Photo provided by Kathy Troost.

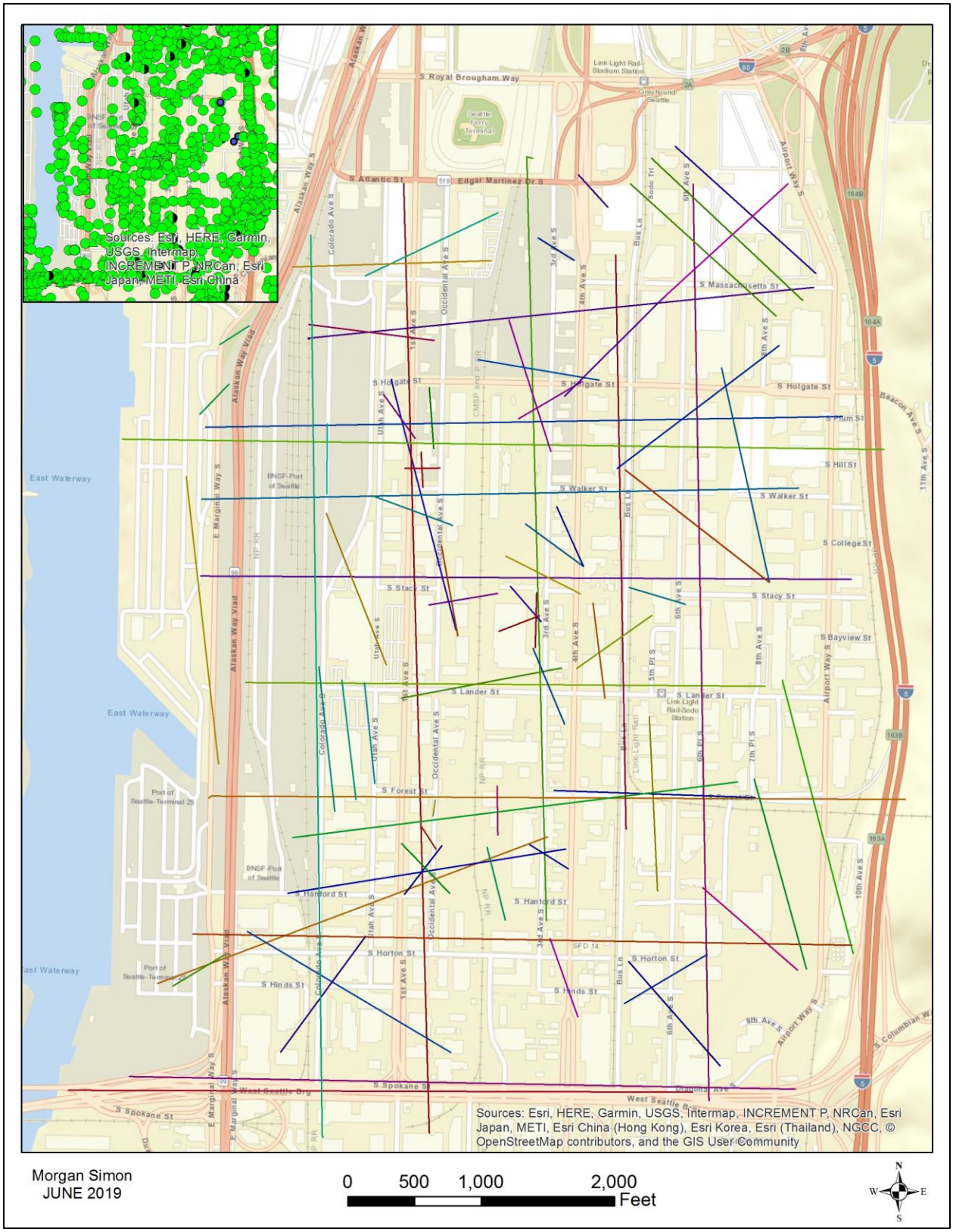

Figure 7- Map showing the locations of the cross-sections lines created to look at the subsurface. Inset map shows the locations of borings in the GeoMapNW database in the study area.

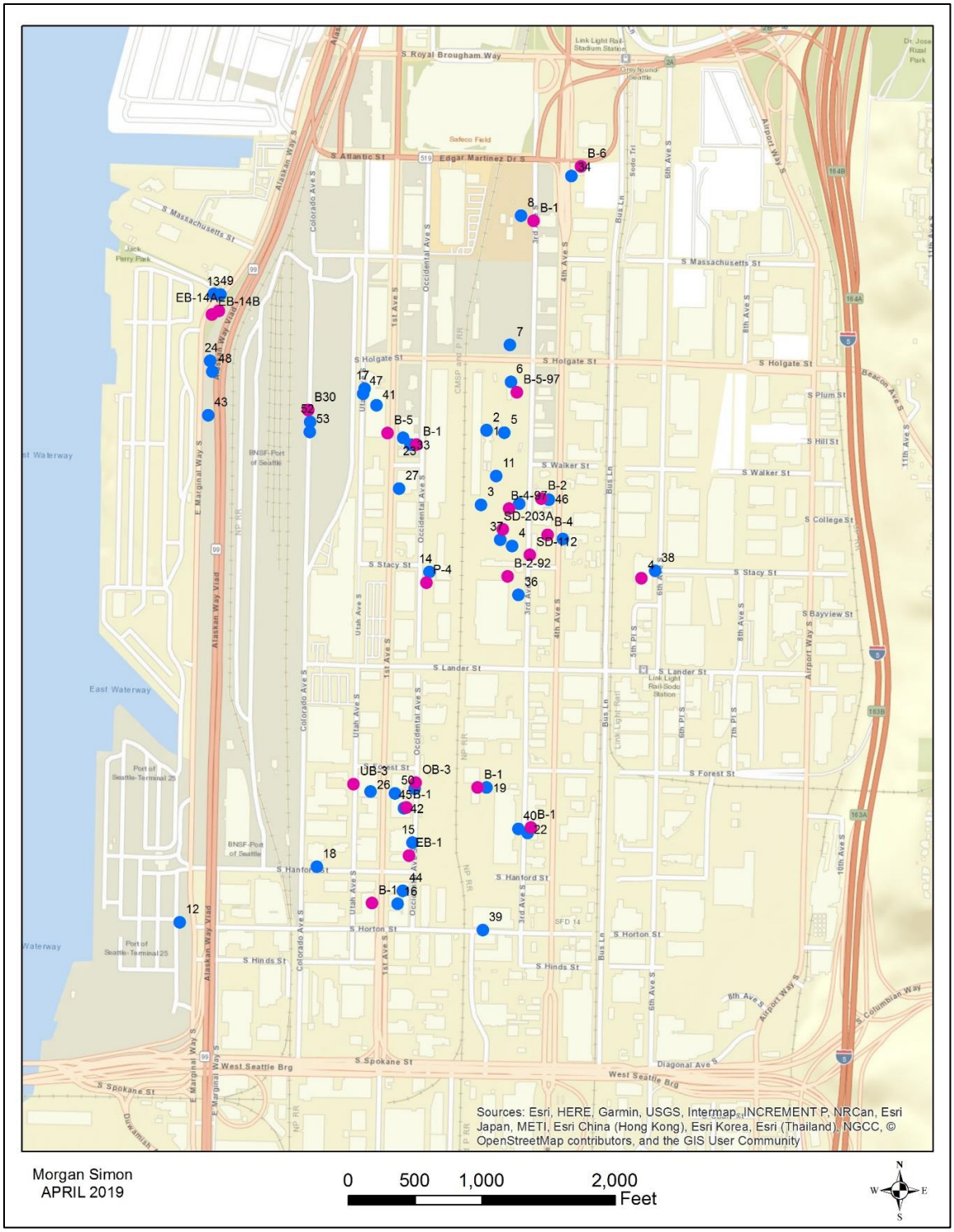

Figure 8- Map showing the locations of sand boils and the borings used to characterize the sand boils. Sand boils are symbolized by the blue dots and are labeled according to the number that they are referred to throughout the text. The borings are symbolized by the pink dots and are labeled by exploration name as recorded in the GeoMapNW database.

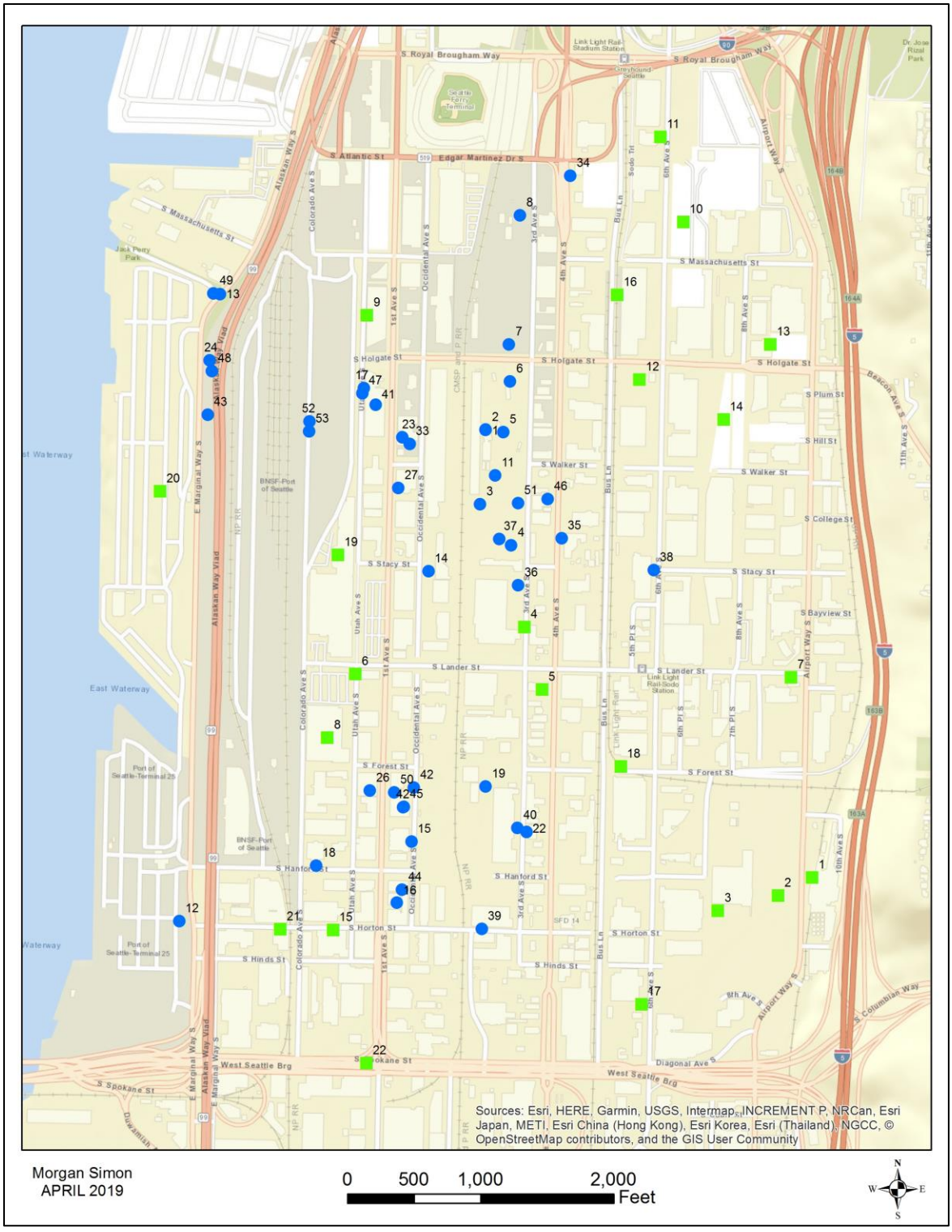

Figure 9- Map showing the locations of sand boils and the boring locations used for characterizing the areas where no sand boils were reported. Sand boils are symbolized by the blue dots and are labeled according to the number that they are referred to throughout the text. Borings for areas without reported sand boils (NSB) are symbolized by the green squares and are labeled according to the number that they are referred to throughout the text.

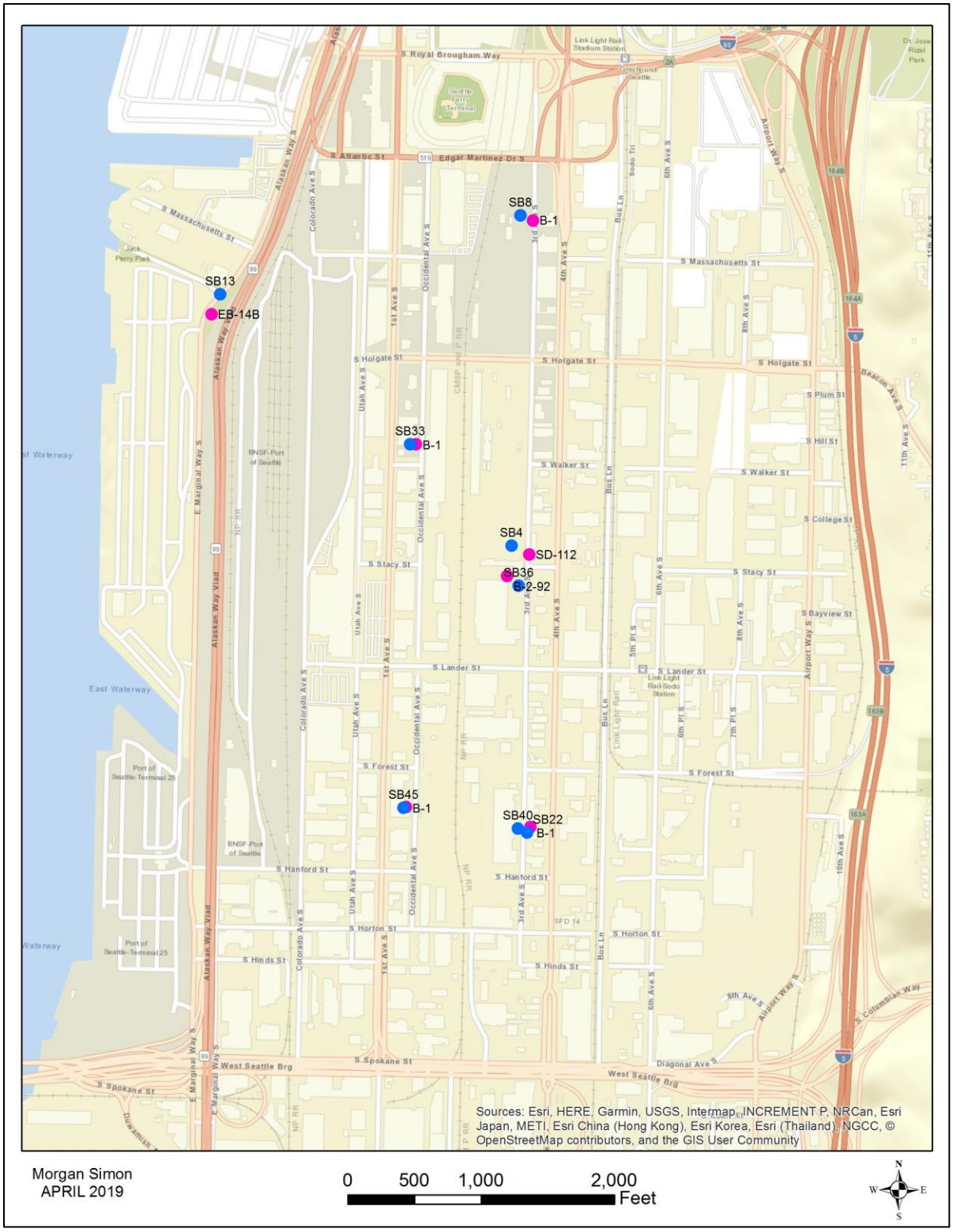

Figure 10- Map showing the locations of sand boils and the borings used to model the sand boils. Clean sand corrections were completed for each of these borings. Sand boils are symbolized by the blue dots and are labeled according to the number that they are referred to throughout the text. The borings are symbolized by the pink dots and are labeled by exploration name.

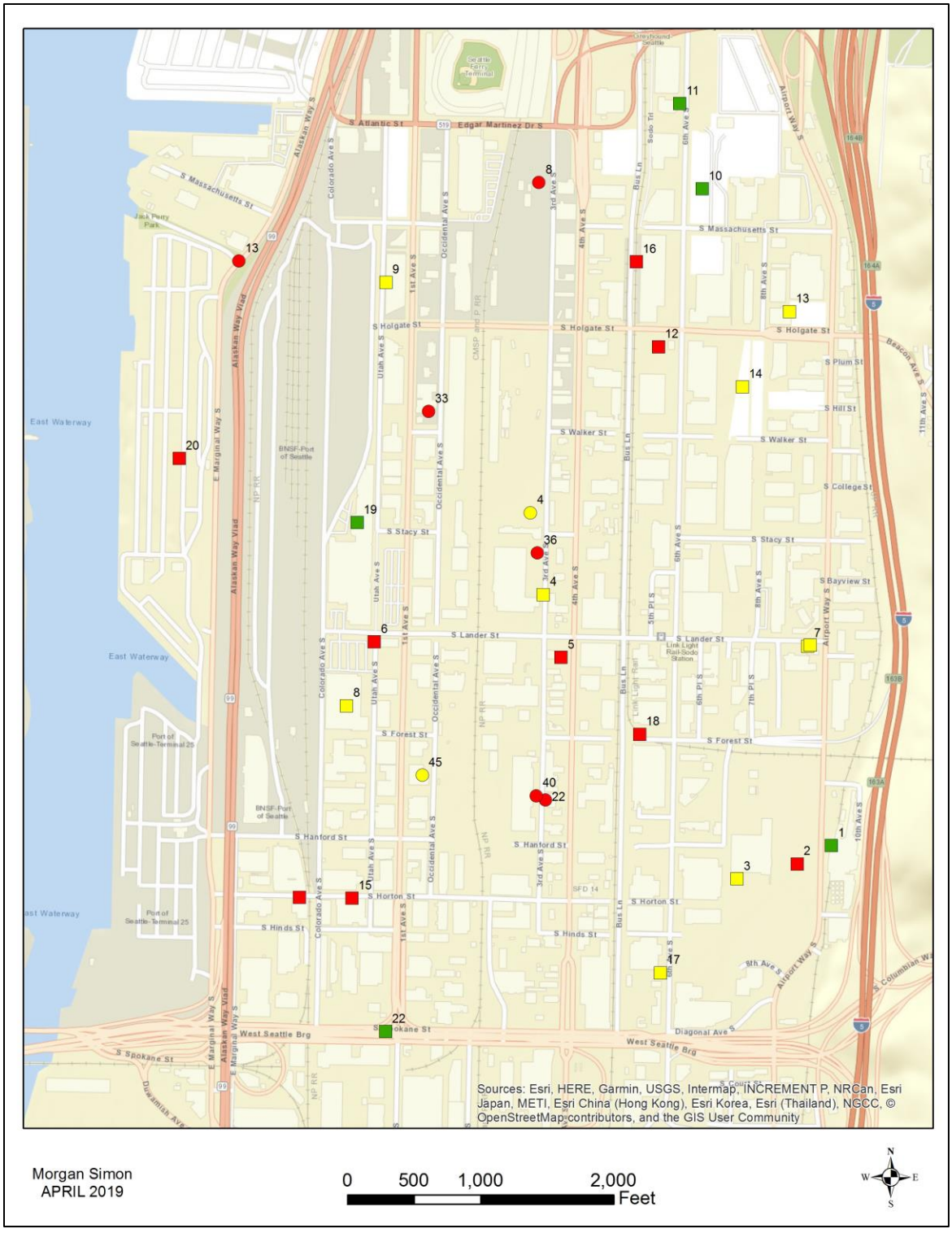

Figure 11- Map showing the LPIs at the boring locations modeled for target locations (sand boils and no sand boils). Clean sand corrections were completed for each of these borings. The squares represent the target locations without reported sand boils and the circles represent the sand boil locations. Green represents a low risk LPI of 0 to 5. Yellow represents a high risk LPI of 5 to 15. Red represents a very high risk LPI of 15 and above.

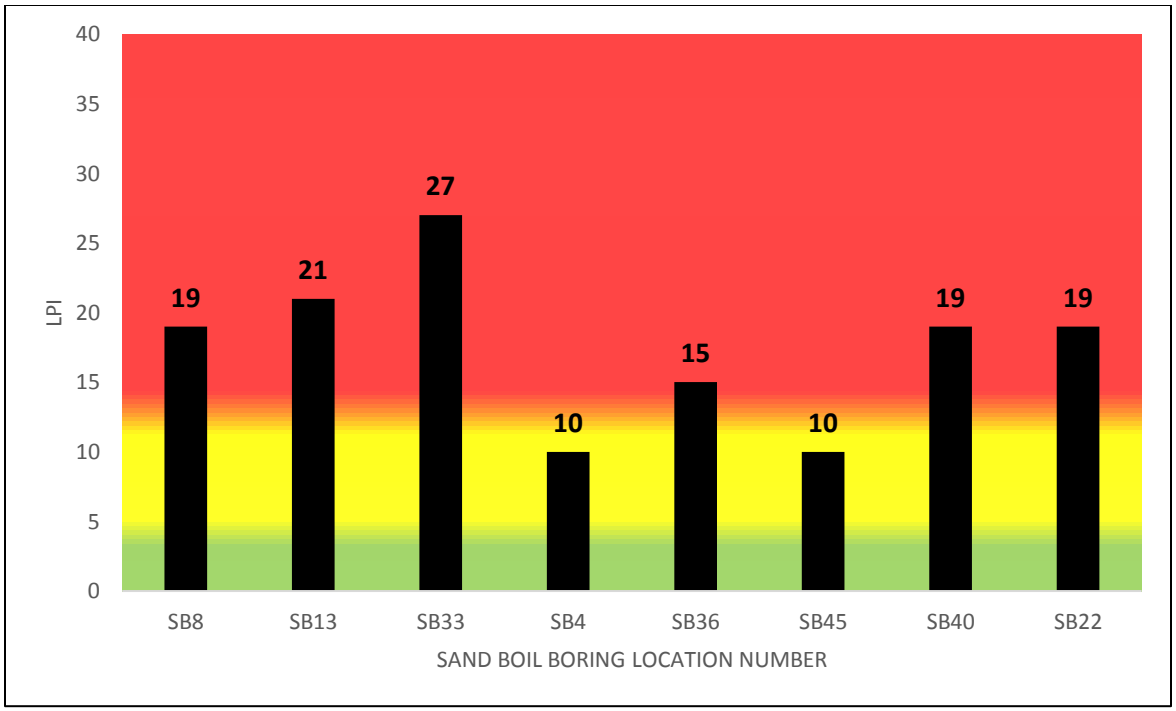

Figure 12- Graph of the LPI for eight sand boil locations (from adjacent borings) from the study area. Organized from north (left) to south (right). Values of 0 to 5 represent low risk, values of 5 to 15 represent high risk and values of 15 and above represent very high risk. Sand boil numbers and locations can be seen on figures 10 and 11.

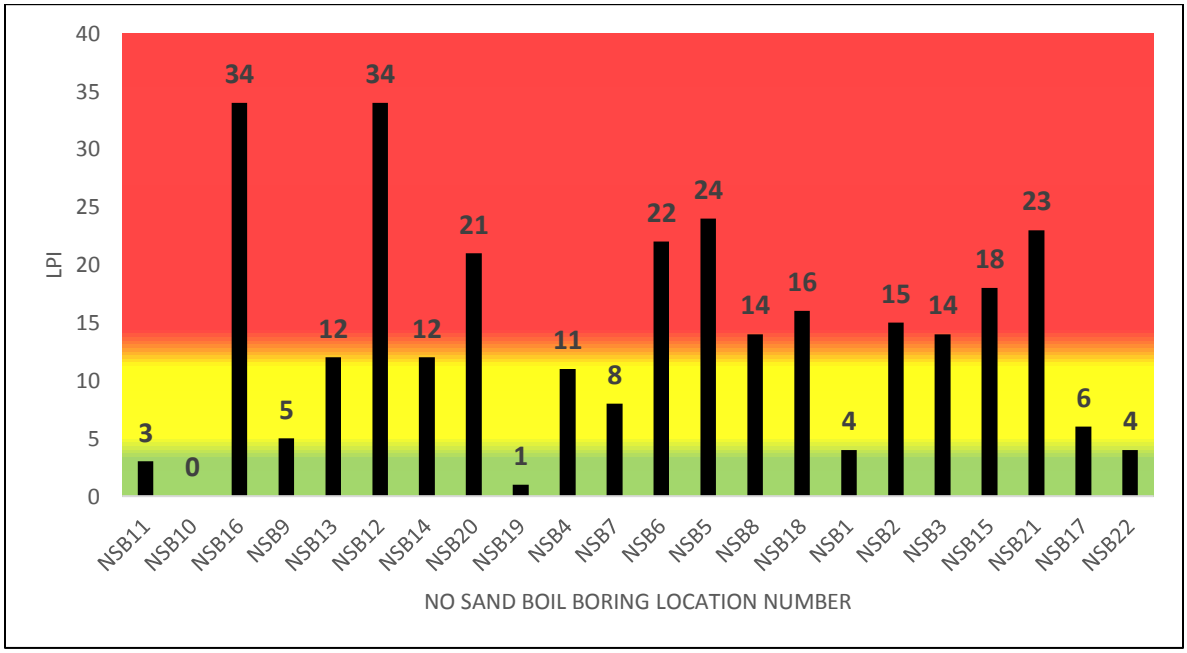

Figure 13- Graph of the LPI for 22 borings where no sand boils were observed in the study area. Organized from north (left) to south (right). Values of 0 to 5 represent low risk, values of 5 to 15 represent high risk and values of 15 and above represent very high risk. Locations can be seen on figures 9 and 11.

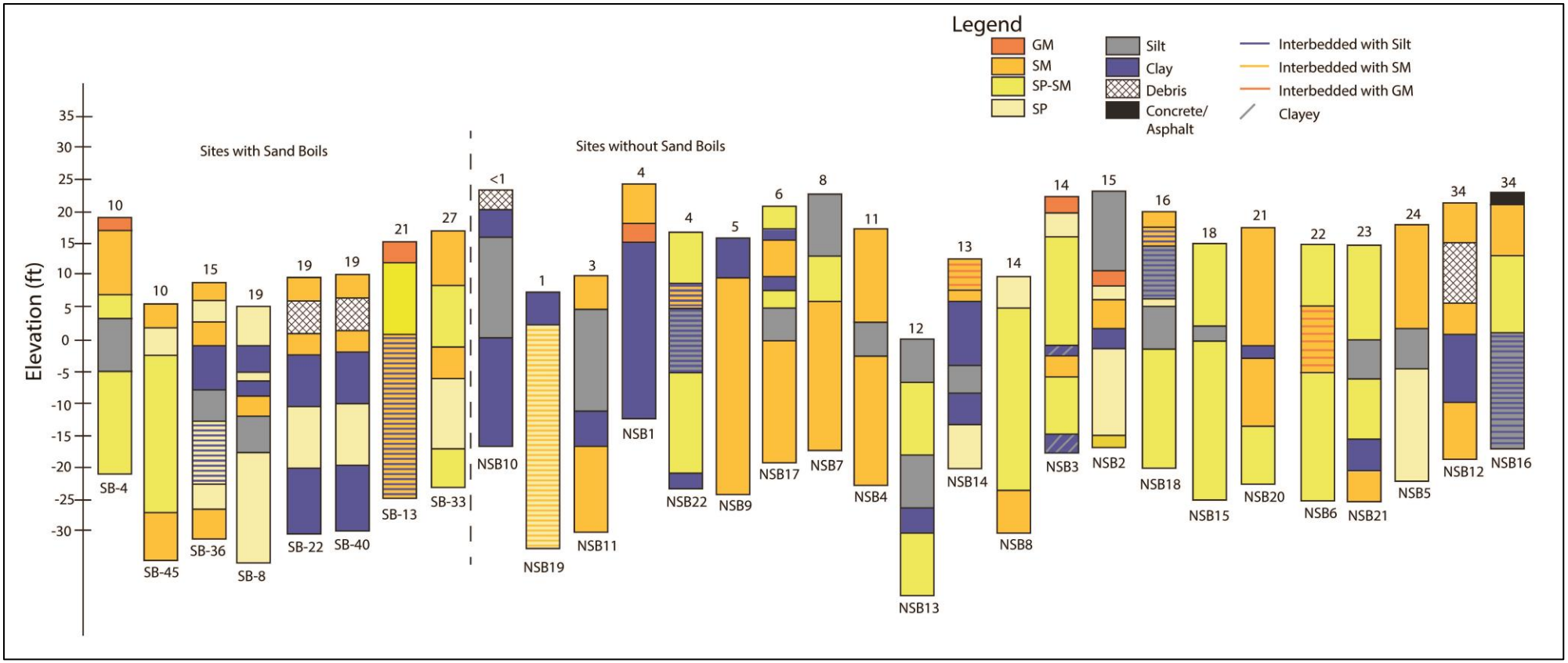

Figure 14- Stick logs of the borings used for modeling the LPI. LPI value is shown at the top of each stick log.

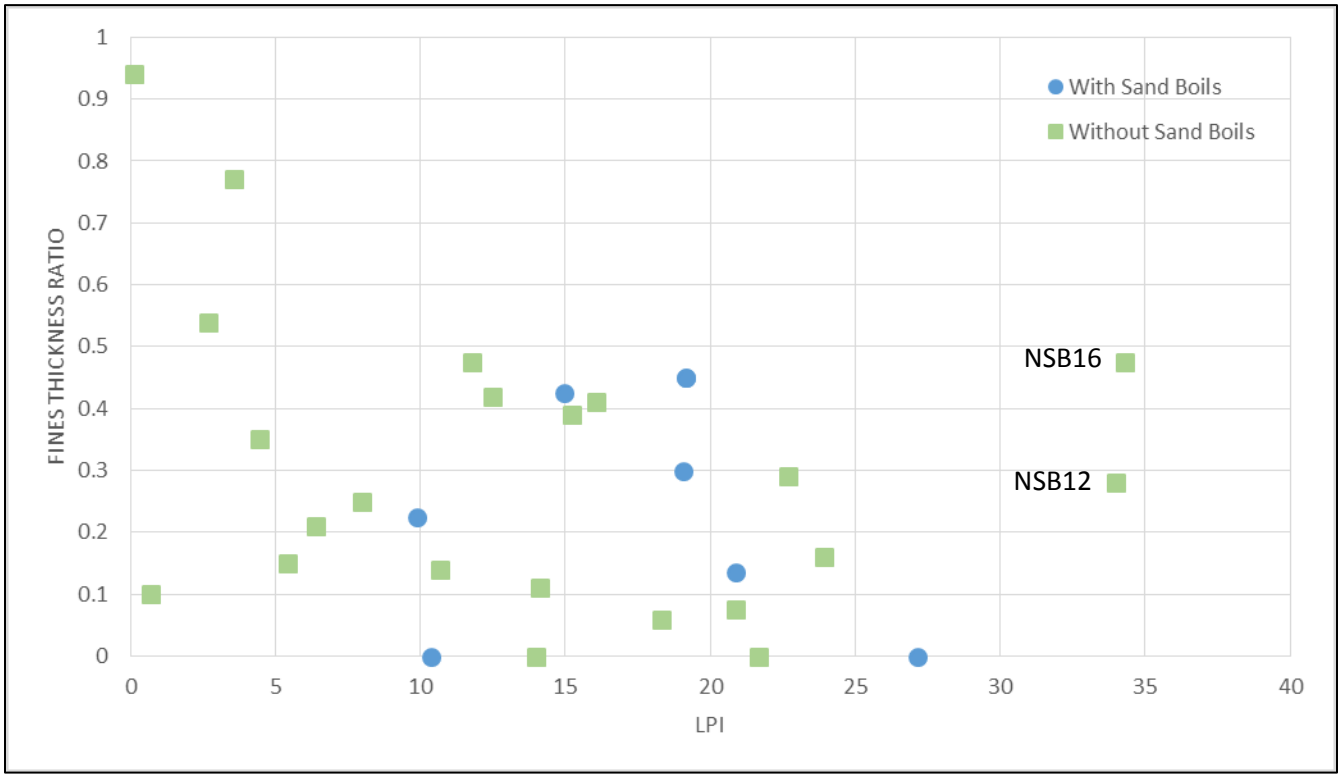

Figure 15- Relationship between LPI and thickness of fines in the upper 40 feet of each boring in target areas. The fines-to-thickness ratio is the ratio of the thickness of fine-grained (silt and/or clay) layers to the total thickness. The blue circles represent sand boils and the green squares represent borings where no sand boils were observed.

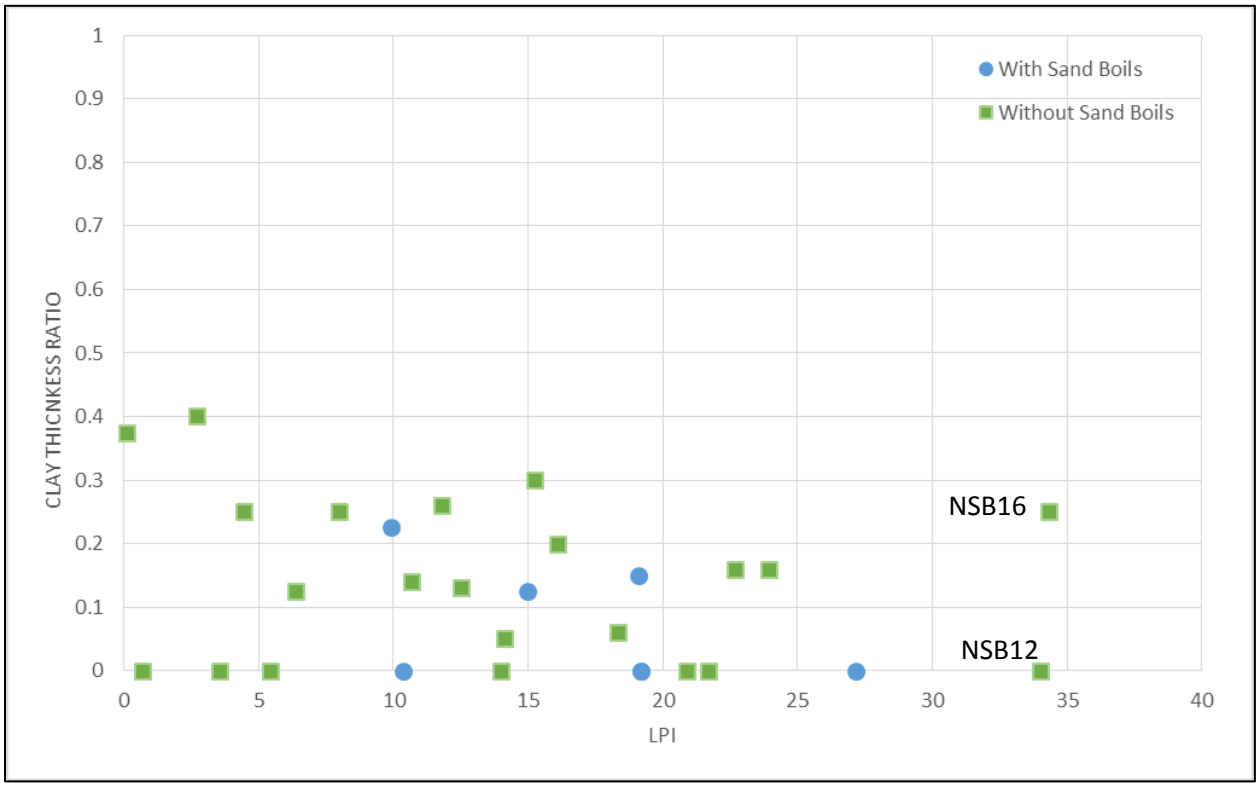

Figure 16- Relationship between LPI and the amount of clay in the top 40 feet of each boring log. The clay to thickness ratio is the ratio of thickness of clay layers to total thickness. The blue circles represent sand boils and the green squares represent borings where no sand boils were observed.

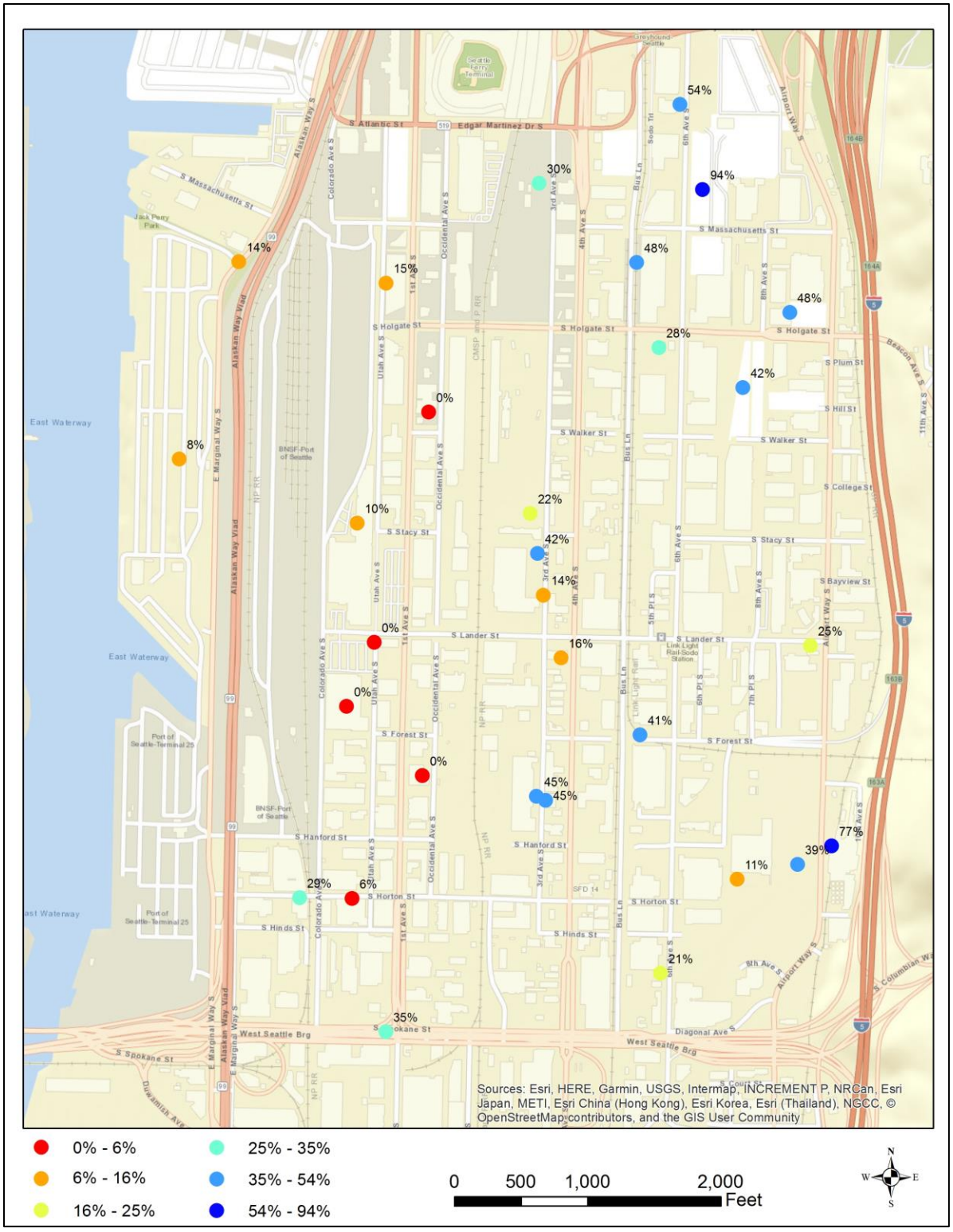

Figure 17- Map showing the percent of fine-grained thickness to total thickness for the upper 40ft at target locations.

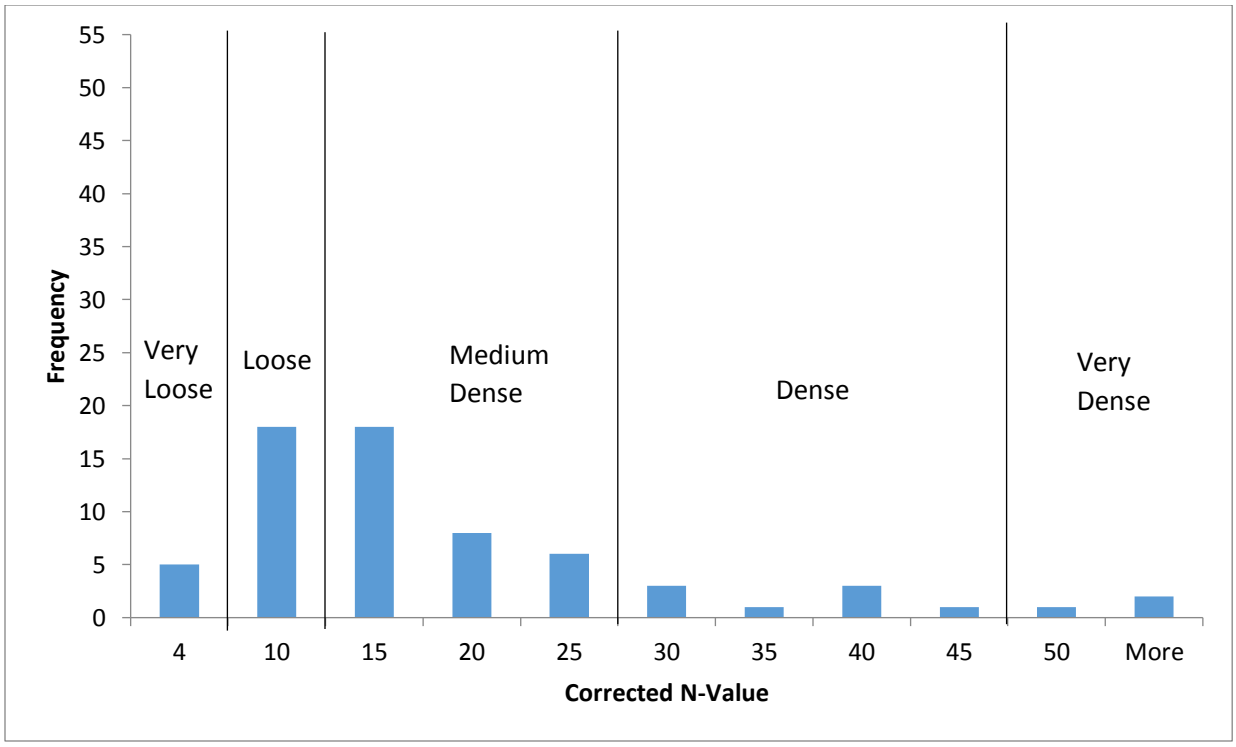

Figure 18- Histogram showing all of the clean-sand-corrected N1(60)cs values from the modeled sand boils. Values below 5 are very loose. Frequency is all N-values from all borings.

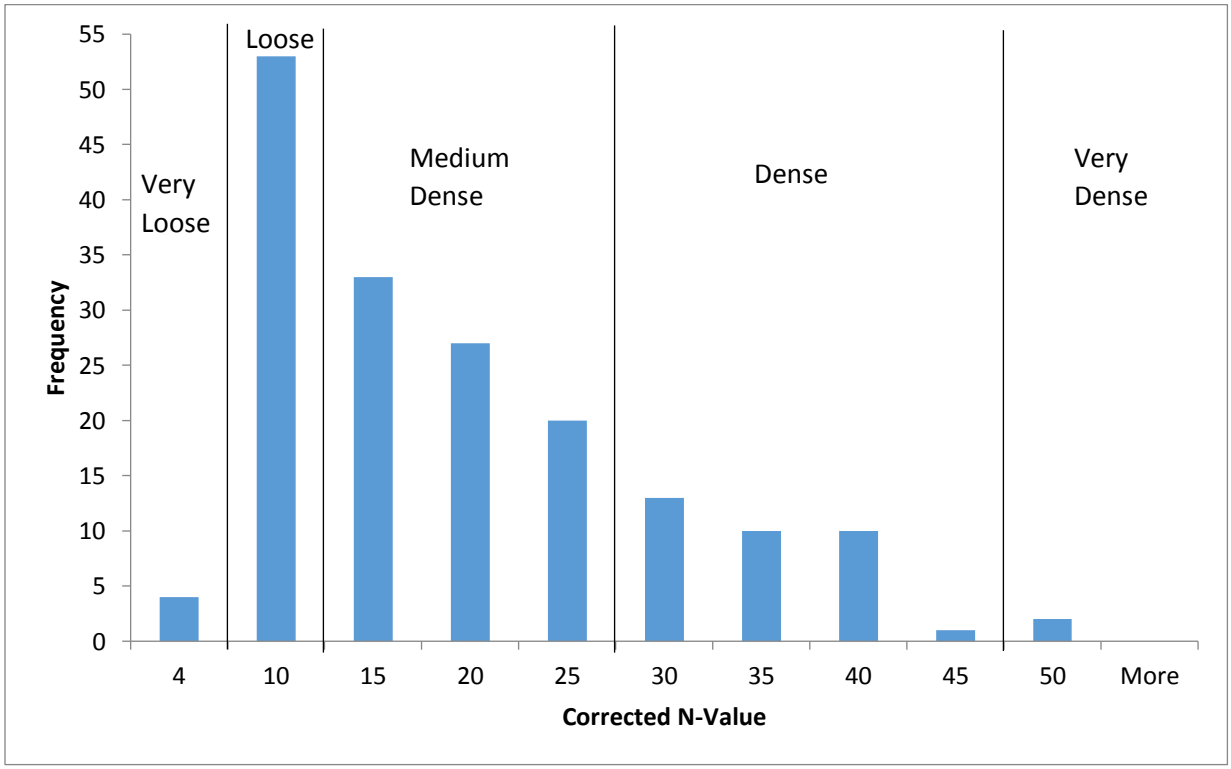

Figure 19- Histogram showing all of the clean-sand-corrected N1(60)cs values from the sites without sand boils. Frequency is all N-values from all borings.

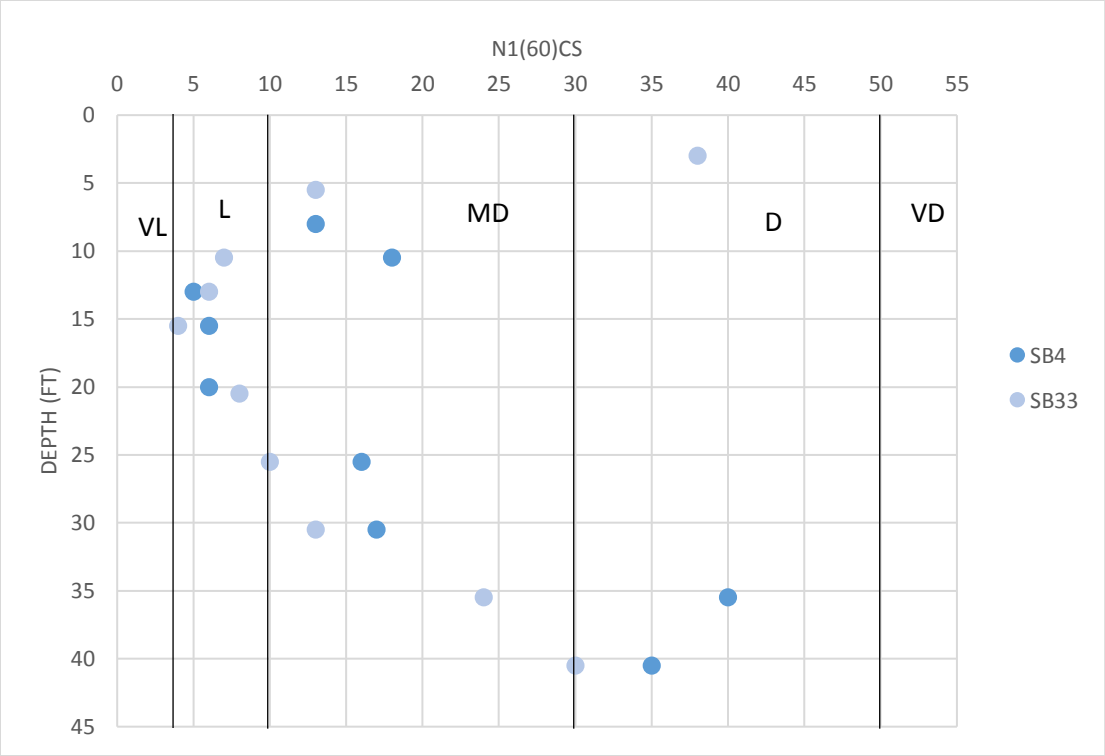

Figure 20- Depth (ft) versus the N1(60)cs density values for borings at Sand Boil 4, which had the lowest LPI and a fine-grained cap, and Sand Boil 33, which had the highest LPI and no fine-grained cap.

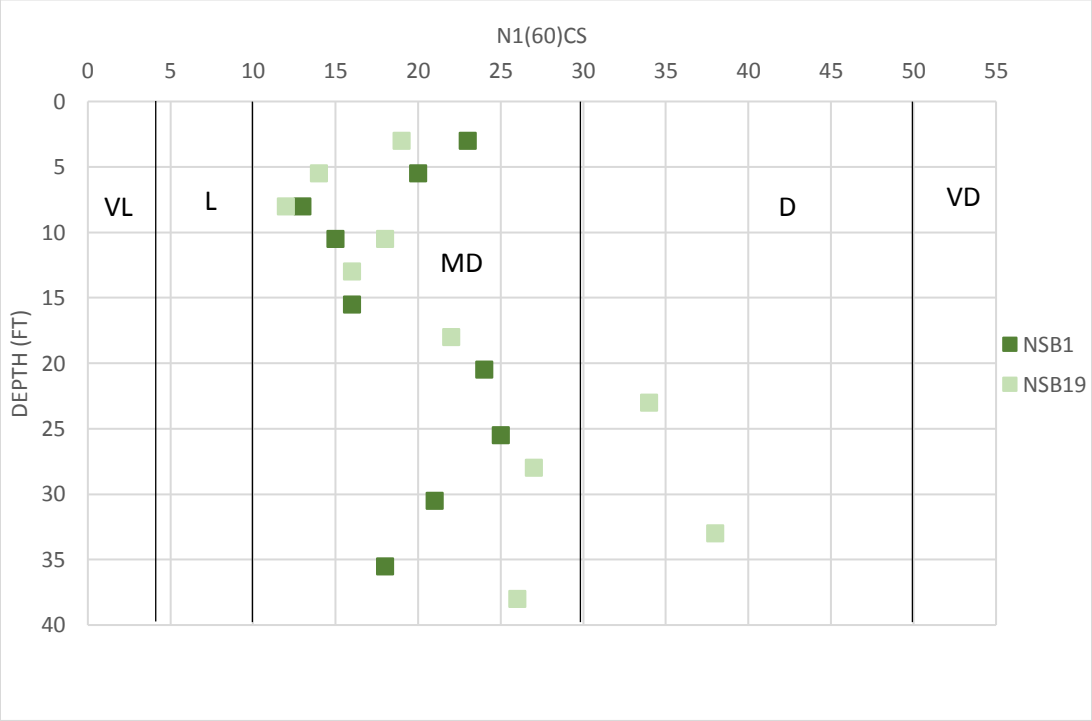

Figure 21- Depth versus the N1(60)cs density values for NSB1, which had a low risk LPI the subsurface consists of mostly silt, and NSB19, which had a low risk LPI and a thin fine-grained cap of silt.

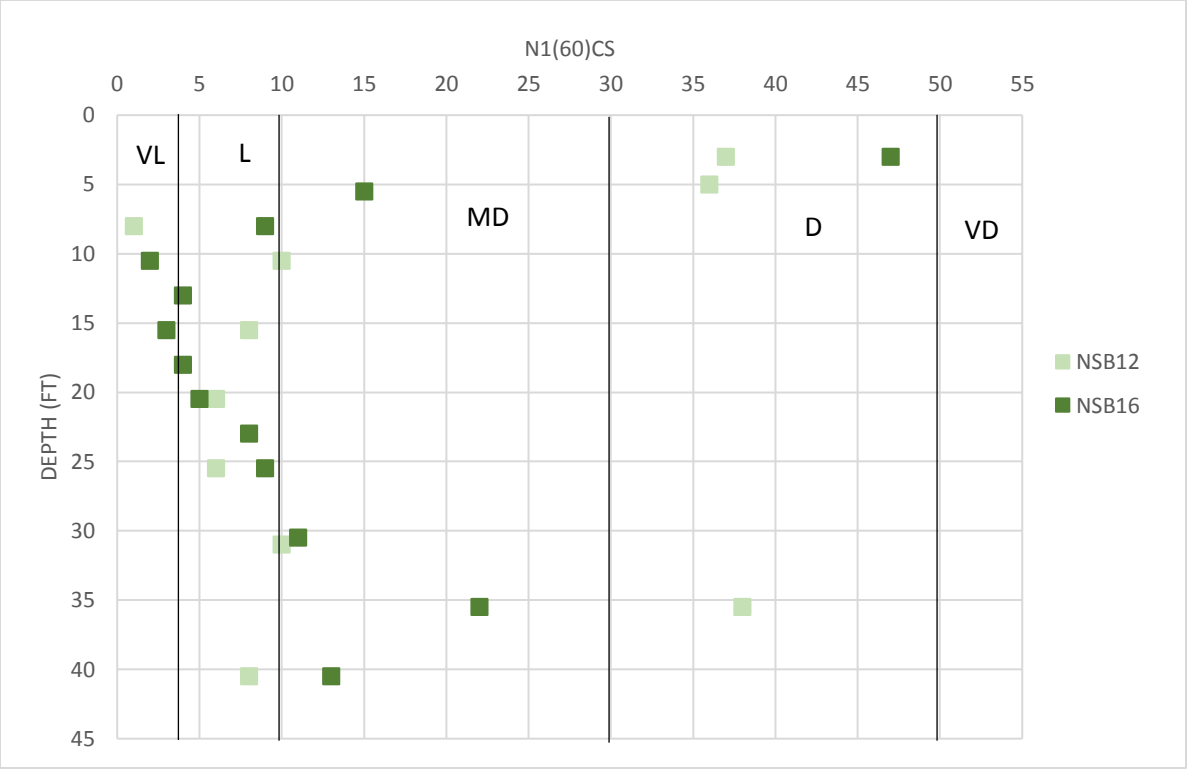

Figure 22- Depth versus the N1(60)cs density values for borings NSB12 and NSB16, both of which have very high risk LPIs and have no fine-grained caps.

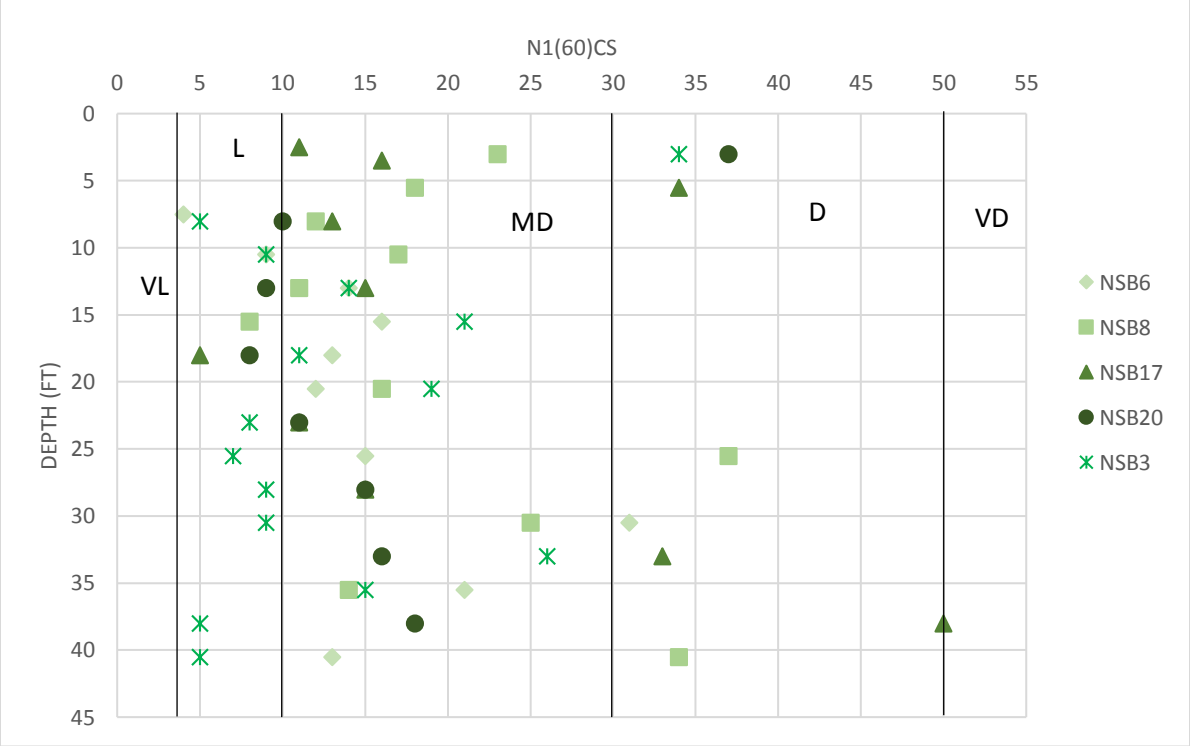

Figure 23- Depth versus the N1(60)cs density values for five additional borings with high or very high LPI and no fine-grained cap.

Appendix A: Equations

Clean Sand Correction: (Boulanger and Idriss, 2014)

$$N_{60} = C_R C_B C_S C_e N$$

$$(N_1)_{60} = C_N N_{60} \tag{2.5}$$

$$C_N = \left(\frac{P_a}{\sigma'_v}\right)^m \leq 1.7 \tag{2.15a}$$

$$m = 0.784 - 0.0768\sqrt{(N_1)_{60cs}} \tag{2.15c}$$

$$\Delta(N_1)_{60} = \exp\left(1.63 + \frac{9.7}{FC + 0.01} - \left(\frac{15.7}{FC + 0.01}\right)^2\right) \tag{2.23}$$

$$(N_1)_{60cs} = (N_1)_{60} + \Delta(N_1)_{60} \tag{2.11}$$

Factor of Safety: (Boulanger and Idriss, 2014)

$$MSF_{max} = 1.09 + \left(\frac{(N_1)_{60cs}}{31.5}\right)^2 \leq 2.2 \tag{2.21}$$

$$MSF = 1 + (MSF_{max} - 1)\left(8.64 \exp\left(\frac{-M}{4}\right) - 1.325\right) \tag{2.19}$$

$$r_d = \exp[\alpha(z) + \beta(z) \cdot M] \tag{2.14a}$$

$$\alpha(z) = -1.012 - 1.126 \sin\left(\frac{z}{11.73} + 5.133\right) \tag{2.14b}$$

$$\beta(z) = 0.106 + 0.118 \sin\left(\frac{z}{11.28} + 5.142\right) \tag{2.14c}$$

$$K_\sigma = 1 - C_\sigma \ln\left(\frac{\sigma'_v}{P_a}\right) \le 1.1 \qquad (2.16a)$$

$$C_\sigma = \frac{1}{18.9 - 2.55\sqrt{(N_1)_{60cs}}} \le 0.3 \qquad (2.16c)$$

$$CSR_{M,\sigma'_v} = 0.65 \frac{\sigma_v}{\sigma'_v} \frac{a_{\max}}{g} r_d \qquad (2.2)$$

$$CRR_{M=7.5,\sigma'_v=1atm} = \exp\left(\frac{(N_1)_{60cs}}{14.1} + \left(\frac{(N_1)_{60cs}}{126}\right)^2 - \left(\frac{(N_1)_{60cs}}{23.6}\right)^3 + \left(\frac{(N_1)_{60cs}}{25.4}\right)^4 - 2.8\right) \qquad (2.25)$$

$$CSR_{M=7.5,\sigma'_v=1} = \frac{CSR_{M,\sigma'_v}}{MSF \cdot K_\sigma} \qquad (2.6)$$

$FS = (CRR_{M=7.5}/CSR)\text{MSF}$

Liquefaction Potential Index: (Iwasaki et al., 1978)

$$LPI = \int_0^{20m} Fw(z)\,dz$$

in which

$F = 1 - FS$ for $FS \le 1$, and

$F = 0$ for $FS > 1$, and

Depth weighting factor, $w(z) = 10 - 0.5z$

Z = Depth

Appendix B: Boring Log Database Tables

Table 5- Boring log inventory for the sites without sand boils. Logs can be found in the GeoMapNW database.

Site Number #	Exploration Name	Exploration ID	Document ID	Date Drilled
NSB1	B-1	16953	2820	9/19/1996
NSB2	GM-10	43244	7829	6/14/2000
NSB3	GM-16	43250	7829	6/28/2000
NSB4	SD-111	62915	11379	8/22/2003
NSB5	B-2	17162	3980	7/28/1999
NSB6	SD-108	62912	11379	8/27/2003
NSB7	B-3	31217	6024	2/18/1988
NSB8	B-5	5413	2209	7/23/1991
NSB9	B-1	10390	3147	8/17/1999
NSB10	EB-6	70507	14370	6/27/2003
NSB11	B-7	70516	14370	9/30/2002
NSB12	B-1	4347	1683	6/1/1995
NSB13	B-1	4883	1980	7/26/1988
NSB14	B-2	72812	15507	9/15/1989
NSB15	SD-104	62907	11379	9/4/2003
NSB16	GC-14	43269	7830	6/19/2000
NSB17	B-101	1229	137	10/27/1989
NSB18	GC-6	43264	7830	5/26/2000
NSB19	B-2	55957	10004	11/27/2000
NSB20	HC-1	55869	9993	9/12/2002
NSB21	SD-103	62906	11379	8/28/2003
NSB22	B-6	45243	8052	6/16/1994

Table 6- Boring log inventory for the sites with sand boils. Logs can be found in the GeoMapNW database. NA means that there was no boring withing vicinity of sand boil.

Sand Boil #	Exploration Name	Exploration ID	Document ID	Date Drilled
SB1	NA			
SB2	NA			
SB3	NA			
SB4	SD-112	62917	11379	8/20/2003
SB5	NA			
SB6	B-5-97	58052	10265	2/3/1997
SB7	B-2-97	58049	10265	1/3/1997
SB8	B-1	45031	8032	5/18/1994
SB11	NA			
SB12	NA			
SB13	EB-14B	61193	11095	3/27/2002

SB14	P-4	2335	644	2/1/1987
SB15	EB-1	70293	14325	12/10/2003
SB16	NA			
SB17	NA			
SB18	NA			
SB19	B-1	45226	8051	10/1/1965
SB22	B-1	1470	236	3/13/1986
SB23	B-5	45339	8053	5/16/1998
SB24	NA			
SB26	UB-3	31225	6024	6/23/1988
SB27	NA			
SB33	B-1	70952	14583	2/7/2002
SB34	B-6	17753	4011	2/13/1984
SB35	B-4	80034	18150	5/1/2002
SB36	B-2-92	49846	9070	1/28/1992
SB37	SD-203A	62931	11379	10/31/2003
SB38	4	33024	6243	5/1/1948
SB39	NA			
SB40	B-1	1470	236	3/13/1986
SB41	NA			
SB42	OB-3	31231	6024	10/7/1988
SB43	NA			
SB44	NA			
SB45	B-1	4601	1835	10/27/1977
SB46	B-2	70134	14213	1/27/2003
SB47	NA			
SB48	NA			
SB49	EB-14A	61192	11095	3/27/2002
SB50	B-1	57885	10236	10/11/2001
SB51	B-4-97	10265	10265	2/4/1997
SB52	B30	14167	3578	2/26/1968
SB53	B30	14167	3578	2/26/1968